Chemical Profiles and Metabolite Study of Raw and Processed Cistanche Deserticola in rats by UPLC-Q-TOF-MSE

Zhe Li
Liaoning University of Traditional Chinese Medicine
Lkhaasuren Ryenchindorj
Drug Research Institute of Mono groups
Bonan Liu
Liaoning University of Traditional Chinese Medicine
Ji SHI (lnshiji@163.com)
Liaoning University of Traditional Chinese Medicine https://orcid.org/0000-0002-6409-4662
Chao Zhang
Liaoning University of Traditional Chinese Medicine
Yue Hua
Liaoning University of Traditional Chinese Medicine
Pengpeng Liu
Liaoning University of Traditional Chinese Medicine
Guoshun Shan
Liaoning University of Traditional Chinese Medicine
Tianzhu Jia
Liaoning University of Traditional Chinese Medicine

Research

Keywords: Cistanche deserticola, Processing, UPLC-Q-TOF-MS E, Chemical profiles, metabolites in vivo

Posted Date: June 3rd, 2021

DOI: https://doi.org/10.21203/rs.3.rs-556141/v1

Chemical profiles and metabolite study of raw and processed *Cistanche deserticola* in rats by UPLC-Q-TOF-MS^{E}

Zhe Li[1], Lkhaasuren Ryenchindorj[2], Bonan Liu[1], Ji Shi[1]*, Chao Zhang[1], Yue Hua[1], Pengpeng Liu[1], Guoshun Shan[1], Tianzhu Jia[1]

(1.Liaoning University of Traditional Chinese Medicine, Pharmaceutic Department, Liaoning Dalian, China;2.Drug Research Institute of Monos Group, Ulaanbaatar 14250, Mongolia)

ABSTRACT:

Background: Chinese materia medica processing is a distinguished and unique pharmaceutical technique in traditional Chinese Medicien (TCM), which has played an important role in reducing side effects, increasing medical potencies, altering the properties and even changing the curative effects of raw herbs.The efficacy improvement in medicinal plants is mainly caused by changes in the key substances through an optimized processing procedure.The effect of invigorating the kidney-yang for rice wine-steamed Cistancha deserticola was more strengthened than raw C. deserticola (CD).

Methods: To evaluate the effect of processing, a comparative analysis was conducted by utilizing the UPLC-Q-TOF-MSE with the UNIFI informatics platform. *In vitro* studies were performed for the characterization of constituents as well as metabolites *in vivo*, and chemical components were determined in CD and its processed products. The multivariate statistical analyses were conducted to evaluate variations between them. OPLS-DA was used for pairwise comparison which revealed their marked differences.

Results: In this study, the obtained results revealed considerable variations in phenylethanoid glycosides (PhGs) and iridoids after processing. The detection of 97 compounds was carried out in the extracts of CD and its processed product. In an in-vivo study, 10 prototype components and 44 metabolites were evaluated in rat plasma, feces, and urine. The obtained results revealed that processing leads to the considerable variation in the chemical constituents of CD and affects the disposition of the compounds in-vivo, and phase II metabolic processes were the key cascades of each compound and most of the metabolites were associated with echinacoside or acteoside.

Conclusions: According to our literature search, the existing study reveals a comparative study of raw and processed CD for the first time. The obtained data help us to understand the impact of CD processing for further studies.

Keywords: *Cistanche deserticola*; Processing; UPLC-Q-TOF-MS^{E}; Chemical profiles; metabolites *in vivo*

1 Introduction

Chinese materia medica (CMM) processing has shown considerable applications in the clinical practice of TCM and for several centuries it has been considered as a potential remedy. This is a unique pharmaceutical technology that has been derived from the theory of Traditional Chinese medicine (TCM). Post-processing, considerable variations have been observed in the appearance, chemical constituents, properties, and medicinal significance of all kinds of TCMs and it has been assumed that processing could promote the efficacy or decrease the toxic effects of the TCM.

For hundreds of years, *Cistanche deserticola* (*Roucongrong* in Chinese, CD) is commonly used in TCM clinical practice, which supplements the functions of the kidney. It also helps in the moisturizing of the intestine that leads to relaxing bowel [1]. The first time, Cistanche was recorded in *ShenNongBencaoJing*. It is commonly occurred in arid and semi-arid habitats across Eurasia and North Africa, including Iran, China, India, and Mongolia [2]. The processing of CD has been carried out by steaming with rice-wine under normal pressure, which is a preparation method documented in the Chinese pharmacopeia (*Jiucongrong* in Chinese, hereinafter called "CD-NP"). And CD steaming with rice-wine under high pressure is a more effective preparation method (hereinafter calling "CD-HP") (hereinafter calling "CD-HP") [3-4]. Several studies have been revealed that the pharmacological effects of CD are different from its processed products [5]. CD may tonify kidney-yang and relax bowel, while after being steamed by rice-wine, the effect of replenishing the kidney-yang would be strengthened. In our earlier study, it has been found that CD-NP could enhance tonification of the kidney and support yang, and relieve the effect of moistening intestines and defecating [6-8]. In clinical practice, the processed products are the most commonly used form.

Up to date, several studies have analyzed the chemical components of CD, followed by isolation and identification of more than 100 compounds [9-11], such as phenylethanol glycosides (PhGs), iridoids, lignans, and oligosaccharides as its main chemical constituents. It has also been reported that there are many pharmacological activities of PhGs including immunomodulatory, neuroprotective, hepatoprotective, anti-inflammatory, and anti-oxidative, etc. [12-14]. Iridoids possess anti-inflammatory activities [15-16]. It has also been revealed by earlier studies that some chemical components showed variations during the processing [17-20]. Based on underlined reports, it has also been considered that post-processing, the variations in chemical composition led to various pharmacological effects, which needs to be further explored.

In the current study, a sensitive and effective method *i.e.,* ultra-high performance liquid chromatography coupled with TOF-MS^E (UPLC-Q-TOF-MS^E) was performed for comparative analysis, and *in-vitro* studies were performed to qualitatively analyze the extracts of CD, CD-NP, and CD-HP which provided clarity in chemical profiles. Generally, the exogenous chemicals with high exposure in target organs were regarded as effective components. Therefore, in rats, CD and its processed products were orally administered respectively, followed by their characterization.

According to our literature search, the existing study reveals a comparative study (both *in vitro* and *in vivo*) of raw and processed CD for the first time. The obtained results would explore our knowledge regarding the effect of CD processing, which might be helpful for further studies.

Materials and Methods

Materials

Ajugol (180120) and standard compounds of 2'-actylacetoside (M0601AS) have been provided by Chendu Pure Chem-Standard Co., Ltd (Chengdu, China). Cistanoside F (MUST-17022620), echinacoside (D1105AS), cistanoside A(M0906AS), and isoacteoside (M0106AS) have provided by Must company (Sichuan China); acteoside (O0618AS), salidroside (J0526AS), catapol (S0728AS), geniposide (A0407AS), and geniposidic acid (MB6001-S) have acquired from Dalian Meilun Bio.Co., Ltd (Dalian, China). 8-Epideoxyloganic acid（B31123）have been obtained from Shanghai Yuanye Biological Technology Co., Ltd, China. Methanol and acetonitrile were of MS-grade and have been obtained from Merck KGaA, Darmstadt, Germany. Methanoic acid (CH_2O_2) of HPLC grade has been provided by Merck KGaA (Darmstadt, Germany). The water, used in the existing study has further been processed via the Milli-Q system (18.2 MΩ, Millipore, Ma, USA). Rice-wine has been provided by Brand Tower Shaoxing Wine Co., Ltd. (Zhejiang, China).

Cistanch deserticola was collected from *Neimenggu wangyedi* cistanche Co. Ltd. The underlined samples have been recognized via Prof. Yanjun Zhai (school of pharmacy, *Liaoning University of TCM*). The specimens have been kept at the *Liaoning University of Traditional Chinese Medicine*.

Animals

Sprague-Dawley male rats (SPF grade) with 180-220 gram of total body weight were provided by Liaoning Changsheng biotechnology Co. Ltd. (Laboratory Animal Resource Center of Liaoning Province, license number: SCXK-2015-0001). These rats were housed in a breeding room with well-maintained temperature, and humidity *i.e.,* 20~26 ℃, 50-70% accordingly for one week. The rats were fed with usual lab food and water before experimentation. The food and water intake were fasted overnight, however, the water ad libitum was provided before the experimentation. The underlined rats were executed via a 10 percent of chloral hydrate anesthetic. The approval for the existing experimentations and protocols was obtained by the Institutional Animal Ethics Committee of Liaoning Provincial Hospital of Chinese Medicine (2019.3.25, 2019015).

Preparation of CD, CD-NP, and CD-HP extract

CD-NP, CD-HP were processed from the same batch of *Cistanch deserticola*. To prepare CD-NP, dry CD sieces (5 mm thick, 100 g) were moisturized by rice-wine (30 mL) and were steamed at 100 ℃ for 16 hrs., followed by drying at 55 ℃ via drying oven. While CD-HP was

prepared via infiltration of dry CD sieces (5 mm thick, 100 g) with rice-wine (30 mL), followed by steaming at high-pressure for 4 hrs. (1.25 atmospheric pressure), dried in a drying oven at 55 ℃ (Liu BN et al).

In a 100 mL measuring flask, one gram of the powder was sieved via sieve#4, followed by adding 50 percent of methanol (50 mL) and then tightly covered and mixed. This mixture was weighed, followed by half hrs. maceration. After maceration, the underlined mixture was ultrasonicate (power 250W, frequency 35kHz) for 40 min, followed by cooling, and weighing again. Replenished the loss of the weight with 50 percent methanol, properly mixed, and allowed to stand, followed by filtering the supernatant and then used the obtained filtrate as the test solution.

MS^E analysis of active components

Preparation of standard substances: precision weighing tubuloside-A, echinacoside, 2'-acetylacteoside, acteoside, isoacteoside, cistanoside-F, salidroside, geniposide, ajugol, catalpol, geniposidic acid, and 8-epideoxyloganic acid of 3.02 mg, 3.00 mg, 2.34 mg, 2.45 mg, 0.61 mg, 2.14 mg, 3.39 mg, 2.84 mg, 1.58 mg, 2.39 mg, 2.56 mg, and 2.34 mg accordingly were added into a 10 mL volumetric flask, added methanol constant volume to scale, configured into a corresponding concentration reference solution. Each of the 100 μL was configured into a mixed reference solution.

MS analysis condition: The mass value was corrected before the experiment, and the negative ion mode was used. The range of mass was 50~1200 Da, and the sample was injected through a flow injection pump. The cone velocity was 100 L/hrs, the dissolvent flow rate was set at 800 L/h. The capillary and cone voltages were fixed at 2500 and 40 V, accordingly. The temperature of the ion source and dissolvent gas were 100 ℃ and 400 ℃, signal acquisition frequency was 0.5 S^{-1}。

UPLC-Q-TOF-MS^E analysis of CD extract

Chromatographic evaluations were carried out in a Waters ACQUITY I-CLASS UPLC system (Waters Corporation, Milford, MA, USA). Including ACQUITY UPLC® BEH C_{18} column (50 × 2.1 mm, 1.7 μm, Waters). The mobile phase was comprised of water having 0.1 percent formic acid (A) and acetonitrile contains 0.1 percent formic acid (B), and the elution condition was as follows: 97% to 85% A (0~1min), 97% to 85% A (1~5 min), 85% to 75% A (5~15 min), 75% to 65% A (15~16 min), 65% to 55% A (16~18 min). The rate of flow and temp of the auto-sampler room and column was fixed at 0.3 $mL \cdot min^{-1}$, 30 ℃, and 8 ℃, accordingly. The injection volume of sample and standard substance solutions was 1 μL.

The mass spectrometric evaluation was carried out via Waters XEVO G2-XS QTOF MS (Waters Corporation, Milford, MA, USA), comprised of an ESI source. The flow rate of nitrogen gas was fixed at 800 $L \cdot hrs^{-1}$ with a temp of 400 ℃, the source temp was fixed at 100 ℃, and the cone gas was set at 50 $L \cdot hrs^{-1}$. The voltage of cone and capillary was adjusted at 40 and 2000 V, accordingly. The collision energy of the ramp was used in the range of 20-30 V. The centroided

data of all samples were obtained from 50-1200 Da, with a 5-scan time of 0.5 s over an analysis time of 10 min. LockSpray TM was employed for the validation of the mass precision. The $[M-H]^-$ ion of leucine enkephalin (200 $pg \cdot \mu L^{-1}$ infusion flow rate 10 $\mu L \cdot min^{-1}$) at *m/z* 554.2615 was used as the lock mass. The MassLynx V4.1 software (Waters Co., Milford, USA) was employed for the accurate mass, the composition of the precursor ions, and the fragment ions calculation.

Data analysis in Masslynx platform

Furthermore, we set up an in-house library comprising the name of the compound, its structure, and molecular formula (in mol.) which is based on literature. All the compounds were noted in a special template, made in Excel. In addition, the mol files (Chemdraw Ultra 8.0, Cambridge soft, USA) and the Excel files of all the individual compound structures were also saved on the local PC. The established Excel-sheet having important data was directly imported into the scientific library in UNIFI.

UNIFI 1.8.2, Waters, Manchester, UK was employed for the evaluation of structural characteristics, particularly for the characteristic fragments and MS fragmentation. The key parameters were adjusted as follows: a minimum peak area of 500 was set for the 2D peak detection. During revealing 3D peaks, a low energy peak intensity of more than 300 counts and elevated energy peak intensity of more than 80 counts were chosen. The error of mass was found to be up to ±10 ppm for known compounds, and the retention time tolerance was set in the range of ±0.1 min. We selected the negative adducts containing -H, +HCOOH. The processing of the raw data obtained from MS was carried out via streamlined UNIFI software to rapidly pinpoint the chemical components that met the standards with the self-built database and the in-house Traditional Medicine Library.

Next, to verify the chemical structure of each target compound, the isomers were distinguished by their characteristic MS fragmentation patterns which were revealed in the reported studies, and by comparing the retention times of reference standards.

Metabolomics Analysis Based on Multivariate Statistical Analysis

Before processing the raw data, the parameters were set, such as mass ranging from 150 to 1200 Da, range of retention time (0 to 20 min), threshold intensity (2000 counts), mass tolerance *i.e.,* 5 mDa, while mass and retention time window was 0.20 min and 0.05 Da, accordingly. In the subsequent list of the database, the identifier of ions was the RT-*m/z* pairs with respect to their elution times. The same values for RT and *m/z* in various batches of samples were considered as the same compound.

Multivariate statistical analysis was conducted to evaluate effective biomarkers that considerably contributed to variations among different groups. During the analysis, principal component analysis (PCA) was employed to indicate the maximum differences and pattern recognition for obtaining an overview and classification. The OPLS-DA is a modeling tool that provides visualization of the OPLS-DA predictive component loading to assist model evaluation.

Variable importance for the projection (VIP) was used for assessing the evaluation of various components, and the metabolites with VIP values > 1.0 and *P-value*<0.05 were regarded as effective markers. Furthermore, a permutation test was conducted for providing reference distributions for the R^2/Q^2 values that could show the statistical significance.

Animal experiments

The rats were randomly categorized into four groups (n=6 for each group), followed by the oral administration of various extracts: (1) Blank control group: the rats were given normal saline (2 mL/100 g); (2) CD group: the rats were given CD extract (2 mL/100 g); (3) CD-NP group: the rats were given CD-NP extract (2 mL/100 g); (4) CD-HP group: the rats were given CD-HP extract (2 mL/100 g). The further categorization of all groups was carried out into three sub-groups for plasma, urine, and feces, accordingly. Two hours later, each rat was orally administered with the same and equal amount of extracts.

Post administration, the collection of blood samples was carried out at 1.0 h, 2.0 h, and 4.0 h in heparinized 1.5 mL polythene tubes (from orbital veins), followed by centrifugation (at 4,500 rpm) of all samples for 15 min. Next, supernatant (200 μL) was taken out and the plasma samples from the same rat were mixed.

For urine and feces samples, the rats were held in metabolism cages, and then the collection of urine and feces samples was carried out for 24 h after administration. The centrifugation of urine samples was carried out at 4,500 rpm for 15 min, while feces samples were dried in the shade, ground into powder, then 0.2 g was taken, and added into 0.5 mL saline solution, then ultrasound for 5 min, and centrifuged at 12000 rpm for 15 min. All the bio-samples were kept at -80 ℃ until analysis.

Preparation of biological samples

The addition of plasma, urine, and feces samples was carried out with 3 volumes of methanol, followed by vortexing for 3 min. Next, the centrifugation (at 12000 rpm) of the mixtures was carried out for 10 min, followed by transferring of supernatant into the EP tube, and then dried by nitrogen at 37 ℃. Furthermore, the addition of 200 μL of HCN-H_2O (50%) solution was carried out. Then, the vortex was used for mixing (1 min), followed by centrifugation (at 12000 rpm) for 5 min. The supernatant (5 μL) of the treated samples was injected into the UPLC-Q-TOF-MS^E system.

Liquid chromatographic and mass spectrometric condition

The analysis for metabolites was also performed by Waters UPLC instrument through an ESI interface. Separations were carried out using an Acquity UPLC HSS T3 column (100 mm×2.1 mm， 1.8 μm), the mobile phase was 0.1 % formic acid (A): Acetonitrile (B), the gradient elution condition was 0~3 min (99.8%→98%A), 3~5 min (98%→95%A), 5~8 min (95%→90%A), 8~12 min (90% →85%A), 12~17 min (85%→70%A), 17~22 min (70%→60%A), 22~23 min

(60%→58%A), 23~25 min (58%A), 25~32 min (58%→45%A), and 32~37 min (45%→35%A), 0.4 mL·min^{-1} was the flow rate. Temperature for column and sample room was set at 40 ℃ and 8 ℃. The above conditions of mass spectrometry were used.

Strategy for systematic analysis of metabolites in bio-samples

UNIFI (1.8.2) software was employed for data processing. The Binary Compare function was used for the identification of effective metabolites. Evaluated metabolites were not existing in the equivalent control sample or exist at low ion intensities. The relative intensity threshold was set at 3 or 5, and metabolites that fulfilled the underlined criteria could be evaluated. Common and predictable metabolites were then determined by EIC. For searching of two-phase metabolites, the NLF function was applied. For example, in the UNIFI software, the parameters could be set at 176.0321 for searching for possible glucuronic acid conjugates. Post-processing, a neutral loss can be set in the method or identified. MassFragment was used for determining or characterization of detected metabolites' structures, a UNIFI's spectral interpretation function is the main function used to analyze secondary fragmentation of parent components. And the underlined function can be used for rapid verification of the fragmentation path whether reasonable.

Results

Mass Fragmentation Rule of Phenylethanoid glycosides and iridoids

Phenylethanoid glycosides are the main chemical constituents of CD. The standard solutions of isoacteoside, cistanoside F, tubuloside A, echinacoside, acteoside, and 2'-actylacteoside were taken, followed by providing a different level of collision energies, and then corresponding MS^2 maps were obtained（Figure 1）.

Table 1 Collision energy for standard substances

Components	Molecular	Theoretical Mass(Da)	Detected Mass(Da)	Fragment	Energy（v）
isoacteoside	$C_{29}H_{36}O_{15}$	623.1976[M-H]$^-$	623.1956[M-H]$^-$	461.1636,315.1636,179.0354,161.0232	35
cistanoside F	$C_{21}H_{28}O_{13}$	487.1452[M-H]$^-$	487.1423[M-H]$^-$	179.0326,135.0440	20
tubuloside A	$C_{37}H_{48}O_{21}$	827.2610[M-H]$^-$	827.2852[M-H]$^-$	665.2477,623.2388,477.1722,161.0202	40
echinacoside	$C_{35}H_{46}O_{20}$	785.2505[M-H]$^-$	785.2651[M-H]$^-$	623.2286，477.1677，179.0374，161.0250	45
acteoside	$C_{29}H_{36}O_{15}$	623.1976[M-H]$^-$	623.2030[M-H]$^-$	461.1691,179.0374,161.0250	25
2'-actylacteoside	$C_{31}H_{38}O_{16}$	665.2082[M-H]$^-$	665.2108[M-H]$^-$	623.1979,503.1784,461.1647,179.0374,161.0250	30
ajugol	$C_{15}H_{24}O_9$	347.1342[M-H]$^-$	347.1410[M-H]$^-$	185.0845,167.0721,149.0624,127.0413	25
catalpol	$C_{15}H_{22}O_{10}$	361.1135[M-H]$^-$	361.1131[M-H]$^-$	199.0586,169.0486,151.0380,125.0332	50
geniposidic acid	$C_{16}H_{22}O_{10}$	373.1135[M-H]$^-$	373.1143[M-H]$^-$	211.0602,193.0500,149.0608,167.0703,123.0453	30
geniposide	$C_{17}H_{24}O_{10}$	387.1291[M-H]$^-$	387.1313[M-H]$^-$	225.0787,207.0678,123.0453	10
8-epideoxyloganic acid	$C_{16}H_{24}O_9$	359.1342[M-H]$^-$	359.1345[M-H]$^-$	197.0810,153.0916,135.0823	40

The mass spectrometric analysis revealed that phenylethanoid glycosides have similar mass spectrum fragmentation patterns, the cleavage pathways in the negative-ion mode mainly include: (1) Ester bond cleavage: loss of neutral caffeoyl group ($C_9H_3O_6$,162.03) and neutral acetyl group

(C_2H_2O, 42.00); (2) Glycosidic cleavage: loss of neutral rhamnose residues ($C_6H_{10}O_4$, 146.05) and neutral glucose residue ($C_6H_{10}O_5$, 162.05). From high-resolution mass spectrometry, caffeoyl (162.03) and glucose residue (162.05) could be distinguished.

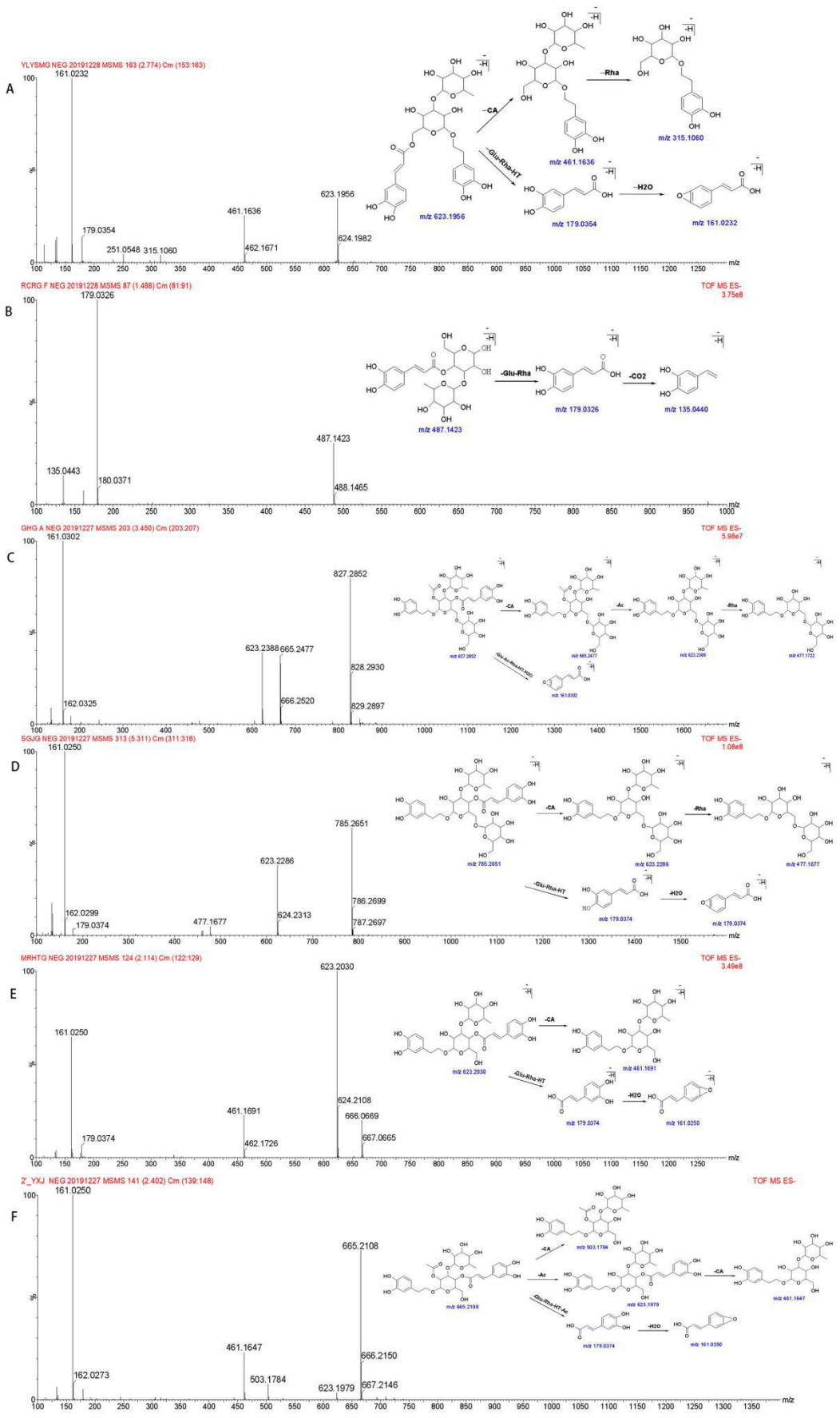
A
YLYSMG NEG 20191228 MSMS 163 (2.774) Cm (153:163)
161.0232
179.0354
251.0548
315.1060
461.1636
462.1671
623.1956
624.1982
m/z
-CA
-Rha
-Glu-Rha-HT
-H2O
m/z 623.1956
m/z 461.1636
m/z 315.1060
m/z 179.0354
m/z 161.0232
B
RCRG F NEG 20191228 MSMS 87 (1.488) Cm (81:91)
TOF MS ES-
3.75e8
179.0326
135.0443
180.0371
487.1423
488.1465
-Glu-Rha
-CO2
m/z 487.1423
m/z 179.0326
m/z 135.0440
C
GHG A NEG 20191227 MSMS 203 (3.450) Cm (203:207)
TOF MS ES-
5.98e7
161.0302
162.0325
623.2388
665.2477
666.2520
827.2852
828.2930
829.2897
-CA
-Ac
-Rha
-Glu-Ac-Rha-HT-H2O
m/z 827.2852
m/z 665.2477
m/z 623.2388
m/z 477.1722
m/z 161.0302
D
SGJG NEG 20191227 MSMS 313 (5.311) Cm (311:316)
TOF MS ES-
1.08e8
161.0250
162.0299
179.0374
477.1677
623.2286
624.2313
785.2651
786.2699
787.2697
-CA
-Rha
-Glu-Rha-HT
-H2O
m/z 785.2651
m/z 623.2286
m/z 477.1677
m/z 179.0374
m/z 179.0374
E
MRHTG NEG 20191227 MSMS 124 (2.114) Cm (122:129)
TOF MS ES-
3.49e8
161.0250
179.0374
461.1691
462.1726
623.2030
624.2108
666.0669
667.0665
-CA
-Glu-Rha-HT
-H2O
m/z 623.2030
m/z 461.1691
m/z 179.0374
m/z 161.0250
F
2'_YXJ NEG 20191227 MSMS 141 (2.402) Cm (139:148)
TOF MS ES-
161.0250
162.0273
461.1647
503.1784
623.1979
665.2108
666.2150
667.2146
-CA
-Ac
-Glu-Rha-HT-Ac
-H2O
m/z 665.2108
m/z 623.1979
m/z 461.1647
m/z 179.0374
m/z 161.0250

A.isoacteoside; B.cistanosideF; C.tubulosideA; D.echinacteoside; E. acteoside; F.2'-actylacteoside

Figure 1 Mass Spectrogram and cleavage pathway of phenylethanoid glycosides

Iridoids ajugol, catalpol, geniposidic acid, geniposide, 8-epideoxyloganic acid standard solutions were taken, followed by providing different collision energies, and then corresponding MS^2 maps were obtained (Figure 2).

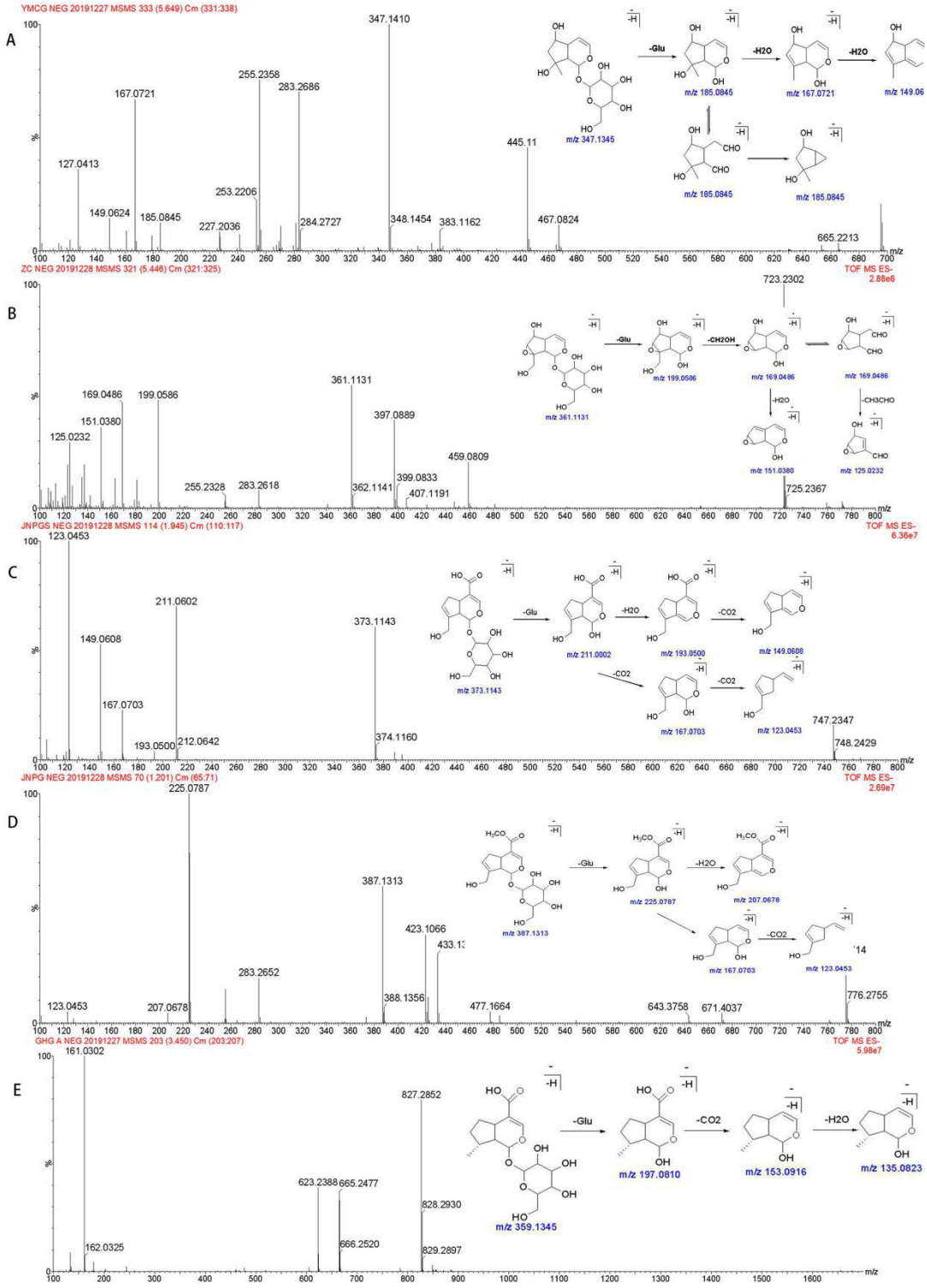

A.ajugol B.catalpol C.geniposidic acid D. geniposide E.8-epideoxyloganic acid

Figure 2 Mass Spectrogram and cleavage pathway of iridoid glycosides

Iridoid glycosides have similar mass spectrum fragmentation patterns, the cleavage pathways in the negative-ion mode mainly include (1) Glycosidic cleavage: Loss of neutral glucose residue ($C_6H_{10}O_5$, 162.05); (2) Loss of neutral CO_2 (43.99) and H_2O (18.01).

Identification of the compounds in CD, CD-NP, and CD-HP extracts

UPLC-QTOF-MS^E analysis

The optimization of chromatographic conditions was carried out. Next, the compounds of Cistanche Herba were evaluated in both negative and positive ion modes with high as well as low CEs. The obtained results revealed that the compatibility of the negative mode was higher relative to the positive mode for the underlined compounds. Figure 1 depicts MS basic peak ion (BPI) chromatogram traced with numbered peaks. The intensity of each detected ion in UPLC-Q-TOF-MS^E analysis was normalized with respect to the whole ion count for the generation of a data matrix which comprised of *m/z* value, the normalized peak area, and retention time.

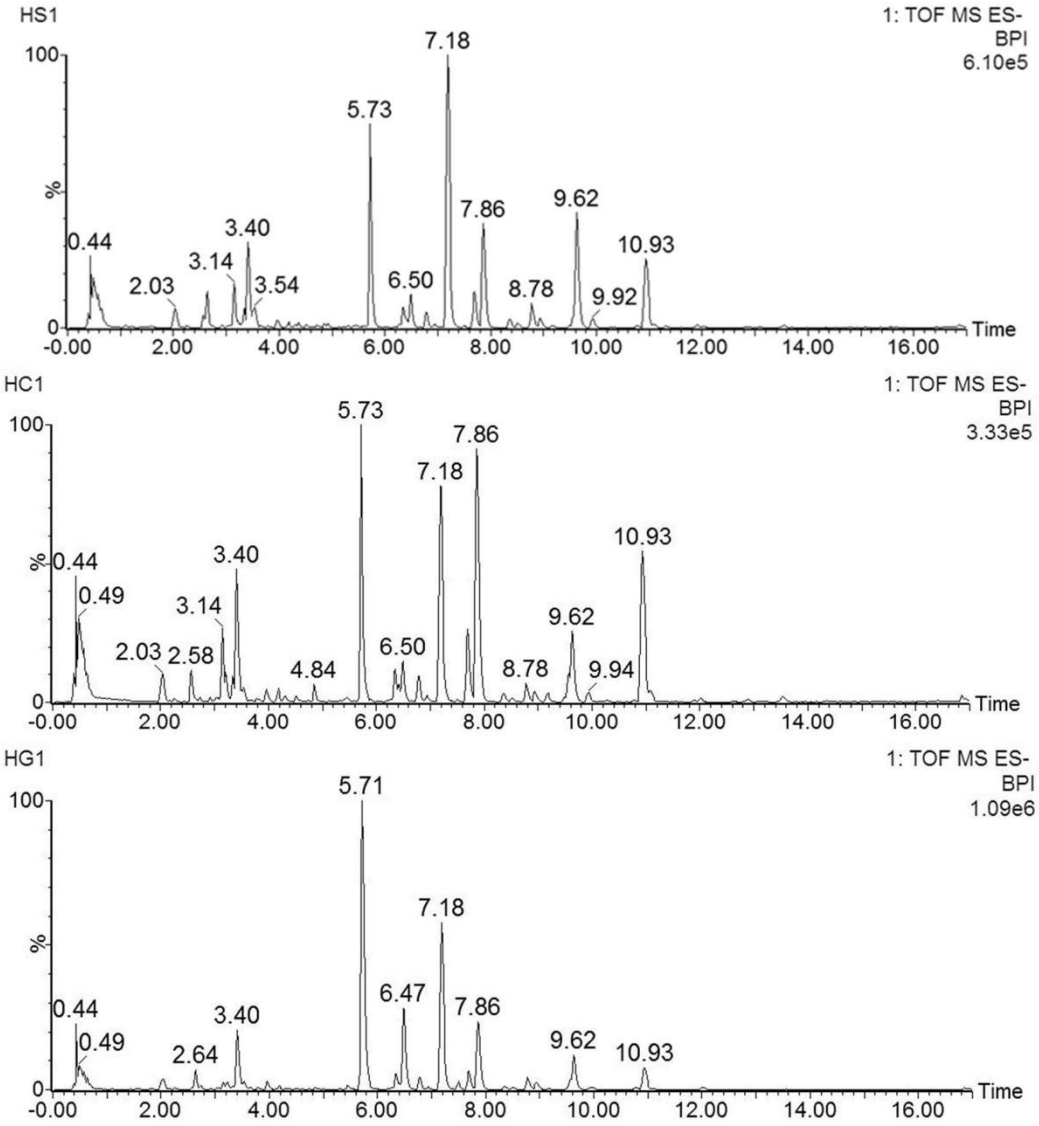

1.CD, 2. CD-NP, 3. CD-HP

Figure 3 The base peak intensity (BPI) of the samples

3.2 The evaluation of components from CD and its processed products on the UNIFI platform

A total of 97 compounds were identified with -SEM (n=6) mode from CD and its processed products (Table 2), including phenylethanoid glycosides (PhGs), iridoids, lignans, and oligosaccharides. The 95, 91, and 94 components were detected in CD, CD-NP, and CD-HP, accordingly. Among them, 64 were phenyaletnanoids, 13 were iridoids, and 20 other kinds of compounds were determined. There was a similarity in the chemical composition of CD and their processed product, however, the quantity of the components was found to be different among CD and its processed product.

Table 2 Evaluation of Compounds obtained from CD and its processed products by UPLC-Q-TOF-MS^E.

NO	RT	Identification	Molecular formula	Adducts	Experimental	Theoretical	Error (ppm)	MS/MS fragmentation	source
1	1.10	Kankanoside B	$C_{15}H_{24}O_{10}$	+HCOO	409.1348	364.1369	0.2	363.12870，183.06693，153.05619	CD，CD-HP
2	1.22	6-Deoxycatalpol	$C_{15}H_{22}O_9$	+HCOO	391.1245	346.1260	0.5	391.12447，341.10886，	CD，CD-NP，CD-HP
3	1.44	6-Deoxycatalpol	$C_{15}H_{22}O_9$	+HCOO	391.1245	346.1260	0.5	391.12448，183.06662	CD，CD-HP
4	2.04	Androsin	$C_{15}H_{20}O_8$	+HCOO	373.1143	328.1163	0.8	373.11434，211.06188，193.05142	CD，CD-NP，CD-HP
5	2.25	6-Deoxycatalpol	$C_{15}H_{22}O_9$	+HCOO	391.1245	346.1260	0.5	391.12446，229.07232，167.03571	CD，CD-NP，CD-HP
6	2.58	Androsin	$C_{15}H_{20}O_8$	+HCOO	373.1147	328.1166	1.2	373.11471，299.11294，211.06206，149.06137	CD，CD-NP，CD-HP
7	2.64	Kankanoside L	$C_{15}H_{24}O_9$	+HCOO	393.1404	348.1421	0.7	393.14046，315.10749，206.06863，134.04736	CD，CD-NP，CD-HP
8	2.93	kankanoside M	$C_{15}H_{22}O_8$	+HCOO	375.1297	330.1318	0.6	375.12966，213.07775，125.06127	CD，CD-NP，CD-HP
9	3.14	3,4-dimethoxybenzyl-β-D-glucoside	$C_{16}H_{24}O_{10}$	-H	375.1299	376.1373	0.8	375.12994，255.08683，213.07767，151.07707	CD，CD-NP，CD-HP
10	3.22	Decaffeoylacteoside	$C_{20}H_{30}O_{12}$	-H	461.1659	462.1734	0	461.16591，315.10891，135.04591	CD，CD-NP，CD-HP
11	3.24	Kankanoside F	$C_{26}H_{40}O_{17}$	-H	623.2192	624.2273	0.5	623.21920，461.16678，315.10994，135.04591	CD，CD-NP，CD-HP
12	3.25	Gluroside	$C_{15}H_{24}O_8$	+HCOO	377.1449	332.1463	0.1	377.14491，461.16609，315.10891，135.04591	CD，CD-NP，CD-HP
13	3.31	Cistantubulose A1	$C_{27}H_{38}O_{18}$	-H	649.1987	650.2068	0.7	649.19871，537.18251，335.09146，179.03598，	CD，CD-NP，CD-HP
14	3.35	6-deoxycatalpol	$C_{15}H_{22}O_9$	-H	345.1193	346.1271	0.7	345.11929，299.11424，179.03598	CD，CD-NP，CD-HP
15	3.40	Adoxosidic acid	$C_{16}H_{24}O_{10}$	-H	375.1302	376.1373	-1.1	213.07683	CD，CD-NP，CD-HP
16	3.54	Cistanoside F	$C_{21}H_{28}O_{13}$	-H	487.1451	488.1532	-0.1	487.14512，325.09503，251.05822，179.03637	CD，CD-NP，CD-HP
17	3.65	Sinapic aldehyde 4-O-β-D-glucopyranoside	$C_{16}H_{20}O_9$	+HCOO	401.1087	356.1109	0.3	401.10872，301.09,397，283.08371，193.05148	CD，CD-NP，CD-HP
18	3.77	Kankanose	$C_{27}H_{38}O_{18}$	-H	649.1985	650.2063	0.5	649.19853，461.16139，293.12495，179.03612	CD，CD-NP，CD-HP
19	3.79	3-Methyl-but-2-en-1-yl-β-D-glucopyranoside	$C_{11}H_{20}O_6$	+HCOO	293.1249	248.1264	1.3	293.12494，195.06673，179.03612	CD，CD-NP，CD-HP
20	3.81	Demethylsyringing	$C_{16}H_{22}O_9$	-H	357.1193	358.1266	0.7	357.11931，251.05778，195.06,678，179.03653	CD，CD-NP，CD-HP
21	3.82	Cistanoside G	$C_{20}H_{30}O_{11}$	-H	445.1709	446.1756	-0.1	445.17092，375.13013，293.12548，195.06823，179.03678	CD，CD-NP，CD-HP

22	3.84	Cistanoside F	$C_{21}H_{28}O_{13}$	-H	487.1458	488.1523	-0.6	487.14577，445.17102,323.08273，179.03678，	CD，CD-NP，CD-HP
23	3.96	3-Methyl-but-2-en-1-yl-β-D-glucopyranoside	$C_{11}H_{20}O_6$	+HCOO	293.1251	248.1268	1.5	293.12505，161.04759	CD，CD-NP，CD-HP
24	3.98	Gluroside	$C_{15}H_{24}O_8$	+HCOO	377.1455	332.1476	0.7	377.14547，293.12505，179.03614	CD，CD-HP
25	4.03	Cistanoside F	$C_{21}H_{28}O_{13}$	-H	487.1457	488.1538	0.5	487.14668，2,23.06196，179.03779	CD，CD-NP，CD-HP
26	4.16	Kankanoside D	$C_{15}H_{26}O_7$	+HCOO	363.1663	318.1679	0.8	363.16634，315.10883，179.03855，161.04465	CD，CD-NP，CD-HP
27	4.19	Cistanoside E	$C_{21}H_{32}O_{12}$	-H	475.1869	476.1888	5.3	475.18694，363.16559，179.03,855	CD，CD-NP，CD-HP
28	4.25	Cistanoside I	$C_{21}H_{28}O_{12}$	-H	471.1505	472.1577	0.2	471.15048，369.11987，471.15071，179.03589，163.04110	CD，CD-NP，CD-HP
29	4.32	Cistanoside F	$C_{21}H_{28}O_{13}$	-H	487.1466	488.153	1.4	487.14656，323.07922，251.05793，179.03699	CD，CD-NP，CD-HP
30	4.53	Cistanoside F	$C_{21}H_{28}O_{13}$	-H	487.1464	488.1537	1.2	487.14637，323.08028，251.05805，179.03769	CD，CD-NP，CD-HP
31	4.55	Androsin	$C_{15}H_{20}O_8$	-H	327.1092	328.1158	1.2	327.10918，251.05805，179.03769，131.07201	CD，CD-NP，CD-HP
32	4.86	Cistanoside H	$C_{22}H_{32}O_{13}$	-H	503.1761	504.1835	-0.4	503.17610，461.16590，375.13036，315.10972，135.04603	CD，CD-NP，CD-HP
33	4.88	Kankanoside E	$C_{16}H_{28}O_8$	+HCOO	393.1760	348.1784	-0.1	393.17603，241.11923，375.13036，161.03814	CD，CD-HP
34	4.92	Cistantubuloside C 1 /C 2	$C_{35}H_{46}O_{21}$	-H	801.2487	802.2556	3.4	801.24867，623.20258，110.03824	CD，CD-NP，CD-HP
35	5.29	(2E,6Z)-2-β-d-Glucopyranosyloxy-2,6-dimethyl-2,6-octadienoic acid	$C_{16}H_{26}O_8$	+HCOO	391.1608	346.1628	0.4	391.16080，345.15509，163.03730	CD，CD-NP，CD-HP
36	5.47	Kankanoside E	$C_{16}H_{28}O_8$	+HCOO	393.1766	348.1783	0.5	393.17656，283.07834，179.03768	CD，CD-NP，CD-HP
37	5.56	Campneoside II	$C_{29}H_{36}O_{16}$	-H	639.1926	640.2003	0.1	621.19264，361.15007，161.02704	CD，CD-NP，CD-HP
38	5.73	Echinacoside	$C_{35}H_{46}O_{20}$	-H	785.2549	786.2618	4.5	785.25485，623.21903，392.11650，179.03596	CD，CD-NP，CD-HP
39	5.81	8-hydroxygeraniol-1-β-D-glucopyranoside	$C_{16}H_{28}O_7$	+HCOO	377.1813	332.1835	0.1	377.18129，331.14023，164.07382	CD，CD-NP，CD-HP
40	5.86	Cistanoside E	$C_{21}H_{32}O_{12}$	-H	475.1813	476.1888	-0.3	347.17188，251.05915	CD，CD-NP，CD-HP
41	5.93	Liriodendrin	$C_{34}H_{46}O_{18}$	+HCOO	787.2670	742.2689	0.9	787.26703，579.20978，475.18047，417.15414	CD，CD-NP
42	6.00	Isolariciresinol-9′-O-β-D-glucopyranoside	$C_{26}H_{34}O_{11}$	+HCOO	567.2076	522.2095	-0.2	567.20755，359.14970，329.13966，178.06231	CD，CD-NP，CD-HP
43	6.06	Campneoside II	$C_{29}H_{36}O_{16}$	-H	639.1936	640.2003	1.1	639.19362，487.14472，251.05630	CD，CD-NP，CD-HP
44	6.26	Kankanosides K 1 /K 2	$C_{36}H_{48}O_{21}$	-H	815.2636	816.2701	2.6	815.26358，783.23518，637.1979，381.15558，179.03631	CD，CD-NP，CD-HP
45	6.34	Cistantubuloside B 1	$C_{35}H_{46}O_{19}$	-H	769.2573	770.2655	1.8	769.25732，623.21303，420.06489，163.03926	CD，CD-NP，CD-HP
46	6.36	8-hydroxygeraniol-1-β-D-glucopyranoside	$C_{16}H_{28}O_7$	+HCOO	377.1820	332.1833	0.8	377.18204，367.15243，163.04196	CD，CD-NP，CD-HP

47	6.42	Kankanoside N	$C_{16}H_{26}O_8$	-H	345.1563	346.1637	1.4	345.15630，197.80891，113.02490	CD，CD-NP，CD-HP
48	6.50	Cistanoside A	$C_{36}H_{48}O_{20}$	+HCOO	845.2769	800.2781	5.4	845.27689，799.27001,681.20502	CD，CD-NP，CD-HP
49	6.47	Kankanoside I	$C_{35}H_{46}O_{18}$	+HCOO	799.2703	754.2718	4.2	799.27031，365.08428，161.02522	CD，CD-NP，CD-HP
50	6.79	(2E,6E)-2-β-D-glucopyranosyloxy-2,6-dimethyl-2,6-octadienoic acid	$C_{16}H_{26}O_8$	-H	345.1565	346.1632	1.6	345.15649，165.09327	CD，CD-NP，CD-HP
51	6.96	Kankanoside A	$C_{16}H_{26}O_8$	-H	345.1565	346.1633	1.6	345.15647，195.06666，179.03628	CD，CD-NP，CD-HP
52	7.03	Cistanoside C	$C_{30}H_{38}O_{15}$	+HCOO	683.2198	638.2208	1.1	683.21978，489.14915，417.15349，335.20636，197.80796	CD，CD-NP，CD-HP
53	7.09	kankanoside E	$C_{16}H_{28}O_8$	-H	347.1716	348.1781	1.0	347.17157，195.81307，167.10929	CD，CD-NP，CD-HP
54	7.19	Acteoside	$C_{29}H_{34}O_{15}$	-H	623.1992	622.1892	1.6	623.19917，461.16657，315.10988，161.02530	CD，CD-NP，CD-HP
55	7.25	Tubuloside A	$C_{37}H_{48}O_{21}$	-H	827.2655	828.2721	4.5	827.26548，621.18343，469.13652，379.19635	CD，CD-NP，CD-HP
56	7.51	Cistanoside B	$C_{37}H_{50}O_{20}$	+HCOO	859.2913	814.2931	4.1	859.2913，679.18910，565.19246	CD，CD-NP，CD-HP
57	7.58	Cistanoside J	$C_{33}H_{42}O_{16}$	+HCOO	739.2409	694.2482	4.0	739.24093，345.15468，161.02597	CD，CD-NP，CD-HP
58	7.60	Tubuloside A	$C_{37}H_{48}O_{21}$	-H	827.2649	828.2727	3.9	827.26486，739.24745，579.22756，345.15468，161.02597	CD-NP，CD-HP
59	7.7	Kankanoside E	$C_{16}H_{28}O_8$	-H	347.1719	348.1791	1.3	347.17191，303.18323，211.13616，185.11917，	CD，CD-NP，CD-HP
60	7.86	Acteoside	$C_{29}H_{36}O_{15}$	-H	623.1995	624.2067	1.9	623.19954，461.16624，161.02546	CD，CD-NP，CD-HP
61	7.94	Crenatoside a	$C_{29}H_{34}O_{15}$	-H	621.1833	622.1907	1.4	621.18331，387.14418，179.03640	CD，CD-NP，CD-HP
62	8.06	Kankanosides K1/K2	$C_{36}H_{48}O_{21}$	-H	815.2631	816.2688	2.1	499.1811，197.8080，160.8423	CD-HP
63	8.33	Kankanoside H1	$C_{37}H_{48}O_{20}$	-H	812.2731	812.2739	-0.8	607.20431，445.17033，161.02556	CD，CD-HP
64	8.36	Isosyringalide-3′-α-L-rhamnopyranoside	$C_{29}H_{36}O_{14}$	-H	607.2034	608.2119	0.7	607.20341，461.16447，315.10906，145.03063	CD，CD-NP，CD-HP
65	8.53	Campneoside I	$C_{30}H_{38}O_{16}$	-H	653.2084	654.216	1.6	607.20440，461.16367，443.15204，145.03081	CD，CD-NP，CD-HP
66	8.78	Cis-isocistanoside C	$C_{30}H_{38}O_{15}$	-H	637.2147	638.2222	1.5	637.21474，475.18074，329.12012，161.02576	CD，CD-NP，CD-HP
67	8.84	Citrusin A	$C_{27}H_{36}O_{11}$	+HCOO	581.2235	536.2280	0.1	581.22351，433.15241,371.13360,343.1457	CD，CD-NP，CD-HP
68	9.17	Isosyringalise-3′-α-L-rhamnopyranoside	$C_{29}H_{36}O_{14}$	-H	607.2033	608.2122	0.6	607.20334，461.15822，161.02611	CD，CD-NP，CD-HP
69	9.50	Isocampneoside I	$C_{30}H_{38}O_{16}$	-H	653.2094	654.2161	1.2	607.2094，461.16616，307.08417，145.03058	CD，CD-NP，CD-HP
70	9.50	Syringalide A-3′-α-L-rhamnopyranoside	$C_{29}H_{36}O_{14}$	-H	607.2037	608.2127	1.0	607.20372，461.16616，307.08417，145.03089	CD，CD-NP，CD-HP
71	9.57	isocistanoside C	$C_{30}H_{38}O_{15}$	-H	637.2150	638.2221	1.8	637.21503，445.15153，323.07862，251.05653	CD，CD-NP，CD-HP
72	9.62	Cis-Tubuloside B	$C_{31}H_{38}O_{16}$	-H	665.2103	666.2169	2.1	665.21032，503.17680，305.06585，161.02529	CD，CD-NP，CD-HP
73	9.76	Crenatoside a	$C_{29}H_{34}O_{15}$	-H	621.1826	622.1891	0.7	621.18264，487.14611，323.07878，179.03579	CD，CD-NP，CD-HP

74	9.92	cistanoside C	$C_{30}H_{38}O_{15}$	-H	637.2139	638.2209	0.7	637.21389，591.20868，445.16991，163.04078，145.03032	CD，CD-NP，CD-HP
75	9.92	Osmanthuside B	$C_{29}H_{36}O_{13}$	-H	591.2080	592.2158	0.2	591.20804，445.16991，160.84291，145.03032	CD，CD-NP，CD-HP
76	10.28	Eutigoside A	$C_{23}H_{26}O_{9}$	-H	445.1501	446.1571	0.2	445.15008，163.03943，145.03004	CD，CD-NP，CD-HP
77	10.35	Cistanoside M	$C_{30}H_{38}O_{14}$	+HCOO	667.2245	622.2248	0.7	667.22446，621.21761，555.20753，161.02534	CD，CD-NP，CD-HP
78	10.78	Isomartynoside	$C_{31}H_{40}O_{15}$	+HCOO	697.2356	652.2372	1.2	697.23563，651.22859，475.17960，175.04062	CD，CD-NP，CD-HP
79	10.92	Salsaside B	$C_{28}H_{34}O_{13}$	-H	577.1929	578.1999	0.8	503.17758，323.07755，161.02527	CD，CD-NP，CD-HP
80	10.93	2′-acetylacteoside	$C_{31}H_{38}O_{16}$	-H	665.2108	666.2173	2.6	665.21076，503.17758，305.06712，161.02527	CD，CD-NP，CD-HP
81	11.08	Osmanthuside B	$C_{29}H_{36}O_{13}$	-H	591.2084	591.2093	0.6	445.1579，163.0400，145.0301	CD，CD-NP，CD-HP
82	11.08	Plantainoside C	$C_{30}H_{38}O_{15}$	-H	637.2141	638.2238	0.9	591.20986，445.15921，145.03022	CD，CD-NP，CD-HP
83	11.33	Kankanosides J1/J2	$C_{32}H_{40}O_{17}$	-H	695.2190	696.2267	0.3	695.21902，649.21477，503.17505，145.03017	CD，CD-NP，CD-HP
84	11.33	SalsasideF	$C_{31}H_{38}O_{15}$	-H	649.2140	650.2199	0.8	649.21399，503.17505，347.16994，145.03017	CD，CD-NP，CD-HP
85	11.89	Cistansinenside A	$C_{32}H_{40}O_{16}$	-H	679.2246	680.2324	0.8	679.22464，623.19749，161.02503	CD，CD-NP，CD-HP
86	12.02	isomartynoside	$C_{31}H_{40}O_{15}$	+HCOO	697.2360	652.2364	1.6	697.23604，651.22862，505.16921，175.04095	CD，CD-NP，CD-HP
87	12.63	Salsaside A	$C_{28}H_{34}O_{13}$	-H	577.1932	578.1982	1.1	577.19316，501.16521，469.13425，179.03540，161.02496	CD，CD-NP，CD-HP
88	12.84	Salsaside Ca/Cb	$C_{28}H_{34}O_{12}$	-H	561.1978	562.2044	0.6	561.19776，415.16021，163.04118，145.03011	CD，CD-NP，CD-HP
89	12.90	SalsasideF	$C_{31}H_{38}O_{15}$	-H	649.2144	650.2212	1.2	649.21443，503.17434，461.16538	CD，CD-NP，CD-HP
90	12.90	Kankanosides J1/J2	$C_{32}H_{40}O_{17}$	-H	695.2195	696.2274	0.8	695.21948，649.21421，607.20459，503.17401，149.02394	CD，CD-NP，CD-HP
91	13.10	Osmanthuside B	$C_{29}H_{36}O_{13}$	-H	591.2085	592.2162	0.7	591.20845，429.17830，161.02556	CD，CD-NP，CD-HP
92	13.11	Jionoside D	$C_{30}H_{38}O_{15}$	-H	637.2131	638.2210	-0.1	591.20842，161.02556	CD，CD-NP，CD-HP
93	13.17	Salsaside D	$C_{31}H_{38}O_{15}$	-H	649.2140	650.2199	0.8	649.21401，607.19810，329.16152	CD，CD-NP，CD-HP
94	13.53	cistansinenside A	$C_{32}H_{40}O_{16}$	-H	679.2251	680.2314	1.3	679.22512，637.21464，461.16791，161.02601	CD，CD-NP，CD-HP
95	14.36	Osmanthuside B6(Z)	$C_{29}H_{36}O_{13}$	-H	591.2085	592.2152	0.7	591.20854，489.26955，445.15395，161.02652	CD，CD-NP，CD-HP
96	15.30	sinenside A	$C_{32}H_{40}O_{16}$	-H	679.2255	680.2328	1.7	679.22547，633.22252，591.20916，145.03024	CD，CD-NP
97	16.43	Cistanoside M	$C_{30}H_{38}O_{14}$	-H	621.2184	622.2258	0.1	591.20868，489.27111，161.02535	CD，CD-NP

Variations in chemical components of processed products

The Simca-P 13.0 software was employed for analyzing the multivariate data matrix. Before PCA, all variables were mean-centered and pareto-scaled, followed by identification of potential discriminant variables. In a PCA score plot, every point showed an individual sample. Samples that showed similarity in their chemical components were scattered adjacent to each other, while those which showed variations in their components were divided. As seen in PCA (Figure 4), the group of CD-HP was separated from the groups of CD and CD-NP.

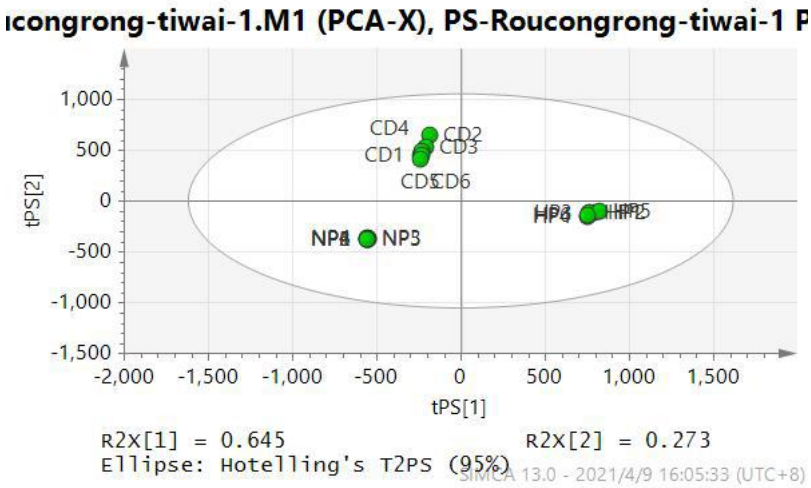

Figure 4 The PCA of CD and its different processed products

To distinguish CD from CD-HP and CD-NP, OPLS-DA, permutation test, S-plot, and VIP value were developed. (Figures 5, 6, 7) The obtained results revealed that many components were key characteristic components of each product. The screening condition was the VIP >1 and $P <$ 0.05. From the date of the S-plot, the characteristic components were evaluated, which were commonly existing in the three groups.

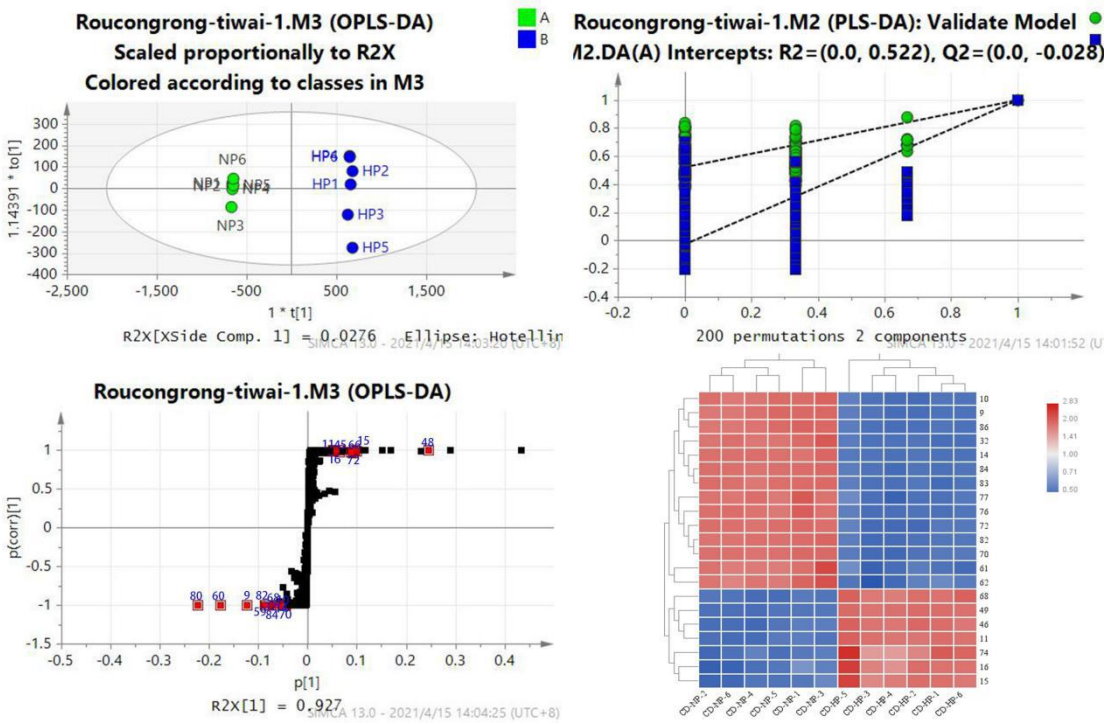

Figure 5 The OPLS-DA/permutation test/S-plot /heat map indicating the intensities of potential biomarkers between CD-NP and CD-HP

Compounds 9, 10, 14, 32, 59, 60, 68, 70, 74, 75, 80, 81, 82, and 84 are the differential components of CD-NP, while compounds 11, 15, 16, 45, 48, 66, and 72 are the differential components of CD-HP.

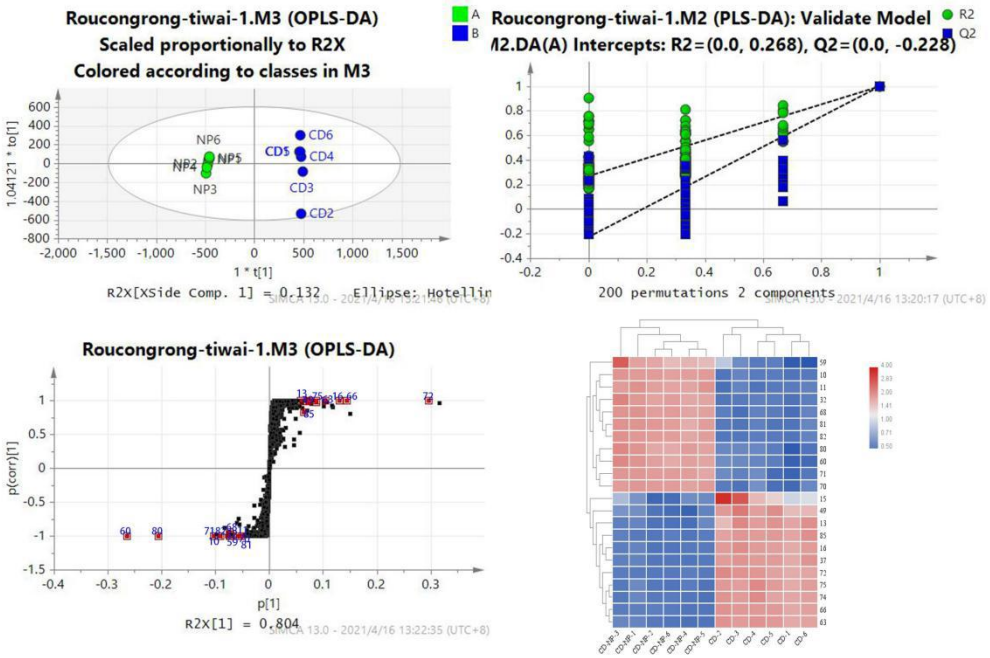

Figure 6 The OPLS-DA /permutation test/ S-plot/ heatmaps indicating the intensities of effective biomarkers between CD and CD-NP

Compounds 13, 15, 16, 37, 49, 63, 66, 72, 74, 75, and 85 are the differential components of CD， while compounds 10, 11, 32, 59, 60, 68, 70, 71, 80, 81, and 82 are the differential components of CD-NP.

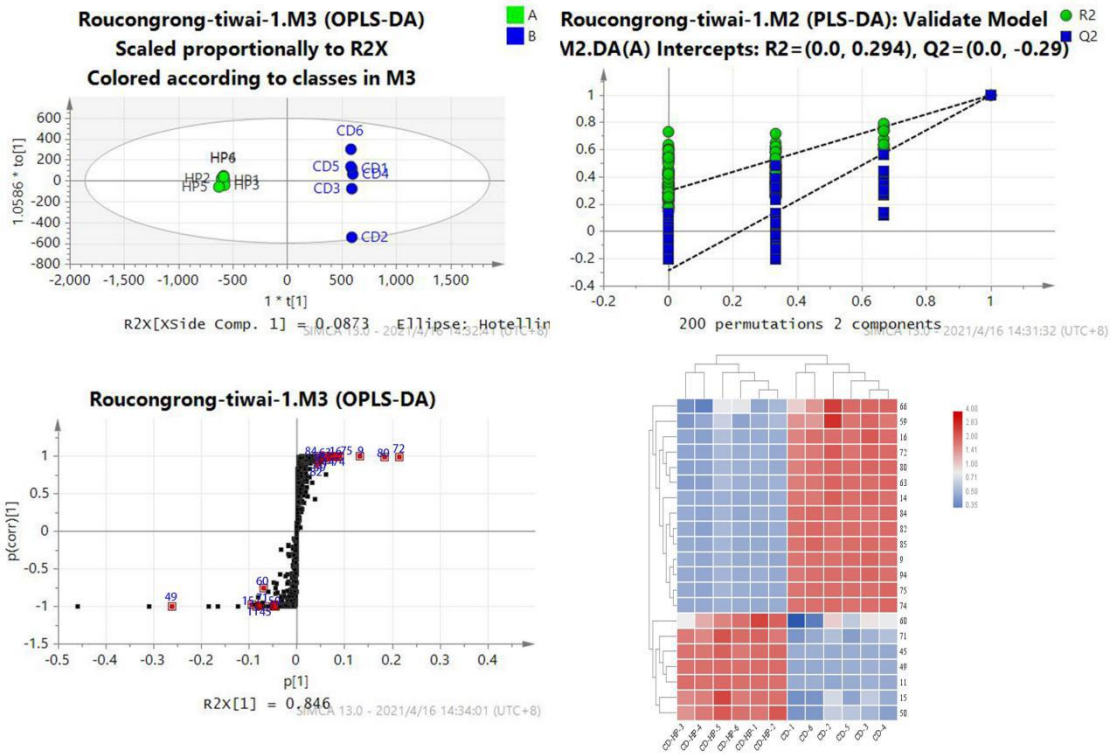

Figure 7 The OPLS-DA/permutation test/S-plot/ heatmaps revealing the intensities of effective biomarkers between CD and CD-HP

Compounds 9, 14, 16, 59, 63, 66, 72, 74, 75, 80, 82, 84, 85, and 94 are the differential components of CD， and 11, 15, 45, 49, 50, 60, and 71 are the differential components of CD-HP.

Identification of the metabolites in rats

From high-resolution mass spectrometry data, the accurate molecular weight and elemental composition for metabolites and protomolecule compounds were analyzed and compared. As the same kinds of compounds in TCM showed similarity in metabolic modifications, the correlations of phytochemical constituents *in-vitro* can extend to their metabolites *in-vivo*. Meanwhile, based on conventional biotransformation pathways, a reasonable change of molecular weight was inferred. Finally, the metabolites were identified by analyzing the MS^E mass spectra of the metabolites and proto-compounds fragmentation pathway in the mass spectrum [21-22].

Compared with the blank sample, its components were identified *in vivo* based on the information provided by chromatogram-mass spectrum, the possibility of a metabolic reaction, the characteristics of the compound structure, and the fragmentation rule of its mass spectrum. See Table 3.

Table 3 Identified Metabolites in serum, urine and feces of aqueous extract in CD and its processed products

NO	**rtmed**	Measured Mass	Error (mDa)	**Formula**	distribution	**Identification**	**status**
1	0.77	179.0389	4.4	$C_9H_8O_4$	$U_{CD,NP,HP}$，$F_{NP,HP}$	Caffeic acid	metabolites
2	0.81	149.0653	5.0	$C_9H_9O_2$	$U_{CD,NP,HP}$	3-phenylpropionic acid	metabolites
3	0.93	195.0623	-3.5	$C_{10}H_{12}O_4$	U_{CD}，S_{NP}，F_{HP}	methylated 3,4-dihydroxybenzenepropionic acid	metabolites
4	1.02	193.0524	2.3	$C_{10}H_{10}O_4$	$U_{CD,NP,HP}$	methylated caffeic acid	metabolites
5	1.18	167.0762	5.4	$C_9H_{12}O_3$	U_{NP}	methylated HT	metabolites
6	3.31	185.117	-0.8	$C_{10}H_{18}O_3$	$U_{CD,HP}$，F_{HP}	Ajugol deglycosylation product	metabolites
7	3.52	167.0536	-0.9	$C_8H_8O_4$	U_{NP}	HT oxidation	metabolites
8	4.48	361.1491	-0.8	$C_{16}H_{26}O_9$	$U_{CD,NP,HP}$，F_{HP}	hydroxylated kankanoside A or isomer	metabolites
9	4.70	541.1144	-8.3	$C_{20}H_{30}O_{15}S$	$S_{NP,HP}$，F_{HP}	decaffeoylacteoside sulfate conjugation	metabolites
10	4.73	153.0504	-4.8	$C_8H_{10}O_3$	$U_{CD,NP,HP}$，$F_{NP,HP}$	HT	metabolites
11	4.85	123.0821	1.1	$C_8H_{12}O$	$U_{CD,NP,HP}$，$F_{CD,HP}$	Geniposide hydrolysated product	metabolites
12	5.14	246.9911	-1.4	$C_8H_8O_7S$	$U_{CD,NP,HP}$，F_{NP}	3,4-dihydroxyphenylacetic acid sulfate conjugation	metabolites
13	5.23	361.1471	-2.8	$C_{16}H_{26}O_9$	$U_{CD,NP,HP}$，$F_{NP,HP}$	hydroxylated kankanoside A or isomer	metabolites
14	5.35	313.0962	3.9	$C_{14}H_{18}O_8$	$U_{CD,NP,HP}$，$F_{NP,HP}$	tyrosol glucuronide conjugation	metabolites
15	5.63	217.0138	-3.3	$C_8H_{10}O_5S$	$U_{CD,NP,HP}$，$F_{NP,HP}$	tyrosol sufate conjugation	metabolites
16	5.73	329.0851	-2.2	$C_{14}H_{18}O_9$	$U_{CD,NP,HP}$	HT-glucuronide conjugation	metabolites
17	5.98	233.0170	-5.0	$C_8H_{10}O_6S$	$U_{CD,NP,HP}$，$F_{CD,NP,HP}$	HT sulfate conjugation	metabolites
18	6.54	185.1114	-6.4	$C_{10}H_{18}O_3$	$U_{CD,NP,HP}$，F_{HP}	deglycosylated kankanoside N	metabolites

19	6.76	261.0084	1.5	$C_9H_{10}O_7S$	$U_{CD,NP,HP}$，F_{NP}	3,4-dihydroxybenzenepropionic acid sulfate conjugation	metabolites
20	7.01	183.1085	6.4	$C_{10}H_{16}O_3$	$U_{CD,NP,HP}$	deglycosylated kankanoside A or isomer	metabolites
21	7.16	461.1605	-5.4	$C_{20}H_{30}O_{12}$	F_{NP}	Decaffeoylacteoside	proto
22	7.19	247.0278	0.1	$C_9H_{12}O_6S$	$U_{CD,NP,HP}$	methylated HT sulfate conjugation	metabolites
23	7.28	345.1476	-7.3	$C_{16}H_{25}O_8$	$U_{CD,NP,HP}$，$S_{CD,NP}$	kankanoside A or isomer	proto
24	7.57	215.0024	0.2	$C_8H_8O_5S$	U_{HP}	HT sulfate conjugation dehydration product	metabolites
25	7.69	355.0704	3.9	$C_{15}H_{16}O_{10}$	U_{HP}，S_{CD}	CA glucuronide conjugation	metabolites
26	7.78	343.1037	0.8	$C_{15}H_{20}O_9$	$U_{CD,NP,HP}$	methylated HT glucuronide conjugation	metabolites
27	7.81	258.994	1.5	$C_9H_8O_7S$	$U_{CD,NP,HP}$	CA sulfate conjugation	metabolites
28	8.19	375.1284	-0.7	$C_{16}H_{24}O_{10}$	$U_{CD,NP,HP}$	8-epilogani acid	proto
29	8.52	245.0125	0.5	$C_9H_{10}O_6S$	$U_{CD,NP,HP}$，F_{HP}	3-HPP sulfate conjugation	metabolites
30	8.53	193.0531	0.8	$C_{10}H_{10}O_4$	$U_{CD,NP,HP}$	Geniposidic acid deglycosylation dehydration product	metabolites
31	8.90	341.0942	6.9	$C_{15}H_{17}O_9$	$U_{CD,NP,HP}$	3-HPP glucuronide conjugation	metabolites
32	9.02	242.9951	-2.1	$C_9H_7O_6S$	$U_{CD,NP,HP}$	dehydroxylated CA sulfate conjugation	metabolites
33	9.06	181.0491	-1.0	$C_9H_{10}O_4$	$U_{CD,NP,HP}$，$F_{CD,NP,HP}$	3,4-dihydroxybenzenepropionic acid	metabolites
34	9.08	151.0352	-4.3	$C_8H_8O_3$	$U_{CD,NP,HP}$	catalpol deglycosylated dehydration product	metabolites
35	9.58	273.0064	-0.5	$C_{10}H_9O_7S$	$U_{CD,NP,HP}$	methylated CA sulfate conjugation	metabolites
36	10.02	275.0209	-1.6	$C_{10}H_{12}O_7S$	$U_{NP,HP}$	methoxylated 3-HPP sulfate conjugation	metabolites
37	10.13	583.1320	-1.3	$C_{22}H_{32}O_{16}S$	$U_{CD,NP,HP}$	Cistanoside H sulfate conjugation	metabolites
38	10.28	299.1108	-2.3	$C_{14}H_{19}O_7$	U_{HP}	salidroside	proto
39	10.4	163.04	0.5	$C_9H_8O_3$	$U_{CD,NP,HP}$，$S_{CD,HP}$，$F_{CD,NP,HP}$	dehydroxylated CA	metabolites
40	10.91	199.0641	3.5	$C_9H_{10}O_5$	U_{NP}	catalpol hydrolysated product	metabolites
41	11.17	521.1816	-5.4	$C_{22}H_{33}O_{14}$	U_{HP}	6-deoxycatalpol glucuronide conjugation	metabolites
42	11.29	165.0558	0.6	$C_9H_{10}O_3$	$U_{CD,NP,HP}$，$F_{CD,NP,HP}$	3-HPP	metabolites

43	11.31	332.1479	0.8	$C_{15}H_{24}O_8$	$U_{CD,NP,HP}$	Gluroside	proto
44	11.31	211.0665	5.8	$C_{10}H_{12}O_5$	$U_{CD,NP,HP}$，$F_{CD,NP,HP}$	deglycosylated geniposidic acid	metabolites
45	12.15	169.0487	-1.4	$C_8H_8O_4$	$U_{CD,NP,HP}$	catalpol deglycosylated product	metabolites
46	12.15	785.2552	4.8	$C_{35}H_{45}O_{20}$	$F_{CD,NP,HP}$	echinacoside	proto
47	13.66	345.1571	2.2	$C_{16}H_{25}O_8$	$U_{CD,NP,HP}$，S_{NP}	6-deoxycatapol	proto
48	13.95	489.1514	-9.4	$C_{21}H_{29}O_{13}$	U_{HP}	cistanoside F reduction	metabolites
49	14.40	487.1480	2.8	$C_{21}H_{27}O_{13}$	$F_{CD,NP}$	cistanoside F	proto
50	14.53	347.1747	-4.1	$C_{16}H_{27}O_8$	$U_{CD,HP}$	kankanoside N	proto
51	14.55	477.1193	-0.4	$C_{23}H_{26}O_{11}$	U_{HP}	calceolarisolide A	proto
52	14.84	315.1174	9.4	$C_{14}H_{20}O_8$	F_{NP}	3,4-dihydroxyphenethyl glycoside	metabolites
53	15.03	197.0833	1.9	$C_{10}H_{13}O_4$	$U_{CD,NP,HP}$	deglycosylation products of 8-epideoxyloganic acid	metabolites
54	16.43	230.9984	1.0	$C_8H_8O_6S$	$U_{CD,HP}$，F_{NP}	4-phenylacetic acid sulfate conjugate	metabolites

Identification of phenylethanol glycosides related metabolites

UNIFI platform was used for processing. Compared with blank samples, a total of 54 metabolites were identified in rats, including 10 prototype components and 44 metabolites, in which 24, 49, and 6 were in feces, urine, and plasma, accordingly.

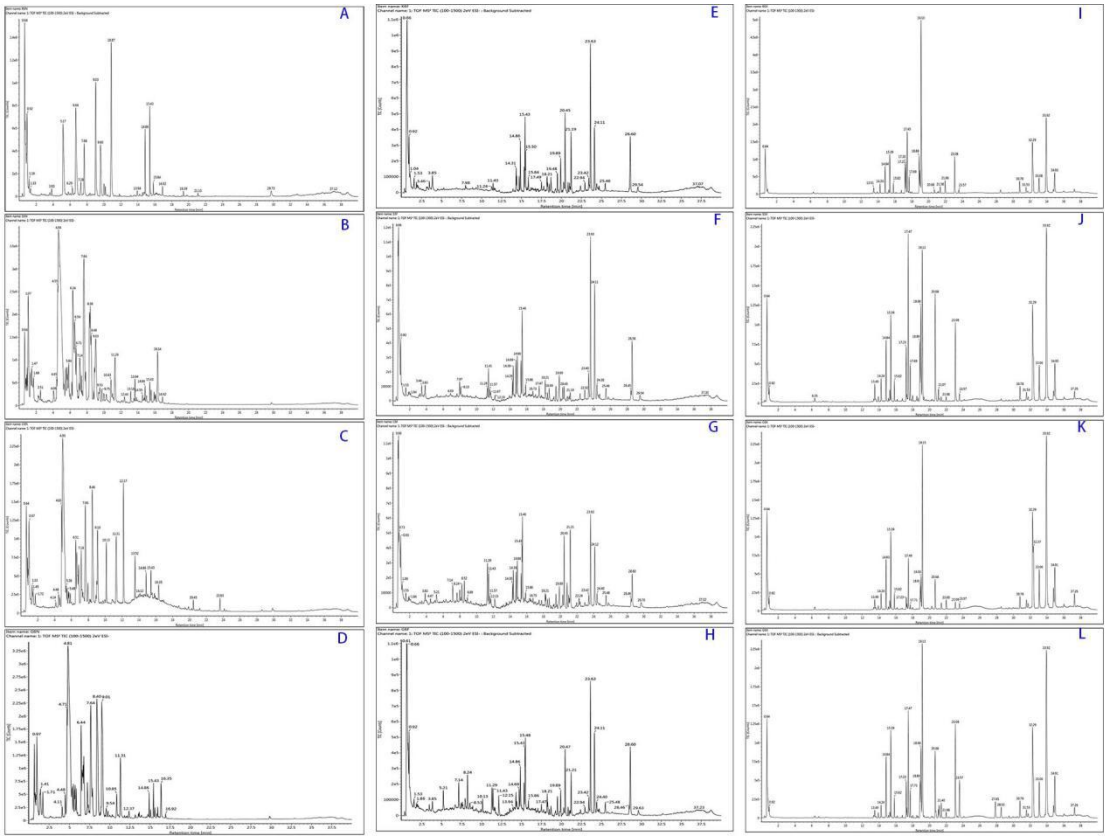

A.Urine sample in BC group; B.Urine sample in CD group; C. Urine sample in CD-NP group; D. Urine sample in CD-HP group; E.Feces sample in BC group; F. Feces sample in CD group; G. Feces sample in CD-NP group; H.Feces sample in CD-HP group; I. Plasma sample in BC group; J. Plasma sample in CD group; K.Plasma sample in CD-NP group; M. Plasma sample in CD-HP group

Figure 8 chromatograph of TIC

Based on accurate mass, fragmentation cascade, and predictable neutral losses by biotransformation, a total of 35 phenylethanoid glycosides-associated metabolites were tentatively evaluated. The related metabolites of phenylethanoid glycosides have similar mass spectrum fragmentation patterns, like the typical decaffeoyl fragment *m/z* 461.1605, then further hydrolyzed by glycosidic and ester bonds *in vivo*, and metabolized into hydroxytyrosol (HT) (*m/z* 153.0504, $C_8H_{10}O_3$, 4.73 min) and caffeic acid (CA)(*m/z* 179.0389, $C_9H_7O_4$, 0.77 min), see Figure 9A.

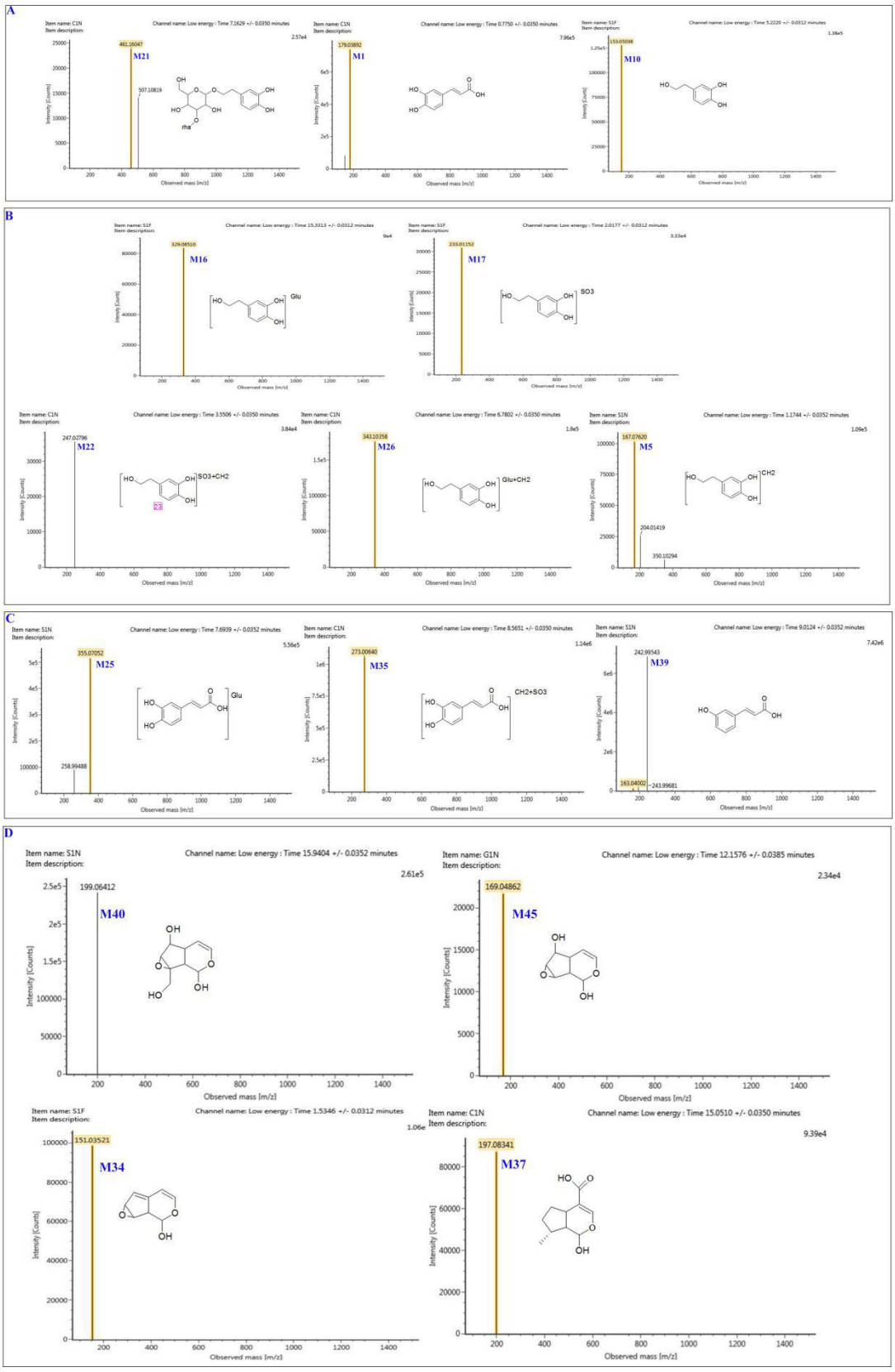

Figure 9 Mass Spectrum of some Metabolites in CDs

M11 indicated $[M-H]^-$ at *m/z* 153.0504 with formula *i.e.,* $C_8H_{10}O_3$, and identified as HT. M16 presented $[M-H]^-$ at *m/z* 329.0851, which was 176 Da elevated than that of HT, revealing that it

might be a glucuronidated metabolite of HT. The $[M-H]^-$ of M26 was at *m/z* 343.1037, 14 Da higher than that of HT-glucuronide. Therefore, M26 was identified as HT-methylated glucuronide. M17 was identified as HT-sulfate based on its $[M-H]^-$ at *m/z* 233.0112, 80 Da over the HT, which could be further methylated, then produced M22, which showed the *m/z* 247.0278, indicating that it was HT-methylated sulfated metabolite. M7 (*m/z* 167.0335) and M5 (*m/z* 167.0762) were considered as oxidation products and methylated HT, respectively. Figure 9B.

M1 indicated $[M-H]^-$ at *m/z* 179.0389, elucidated molecular formula was $C_9H_7O_4$ and identified as caffeic acid (CA). M25 revealed $[M-H]^-$ at *m/z* 355.0704, which were 176 Da elevated than that of CA, shows that it might be a glucuronidated metabolite of CA. M27 had *m/z* 258.994, which was 80 Da higher than that of CA, so we elucidated it as CA sulfate, and it could produce M35 (*m/z* 273.0064). As M4 gives the $[M-H]^-$ at *m/z* 193.0524, 14 Da higher than CA, it was identified as CA methylated metabolite. M39 was CA dehydroxylation metabolite, whose *m/z* 163.04, it could be sulfated into M32 (*m/z* 242.9951).

M33 (*m/z* 181.0491, $C_9H_{10}O_4$, 9.06 min) was the reduction product of CA, that is 3,4-dihydroxybenzenepropionic acid, which could be methylated into M19 (*m/z* 195.0623, $C_{10}H_{12}O_4$, 0.93 min). M33 could be dehydroxyed into M43, that is 3-HPP (*m/z* 165.0558, $C_9H_{10}O_3$, 11.29 min), and M31 (*m/z* 341.0942, $C_{15}H_{17}O_9$, 8.90 min) and M29 (*m/z* 245.0125, $C_9H_{10}O_6S$, 8.52 min) were the glucuronidated and sulfated products. Figure 9C.

For the phenylethanoid glycosides-associated metabolites, the key metabolic cascades were phase II metabolic reactions, *i.e.,* glucuronidation, methylation, and sulfation. The proposed metabolic cascades of phenylethanoids are depicted in Figure 10.

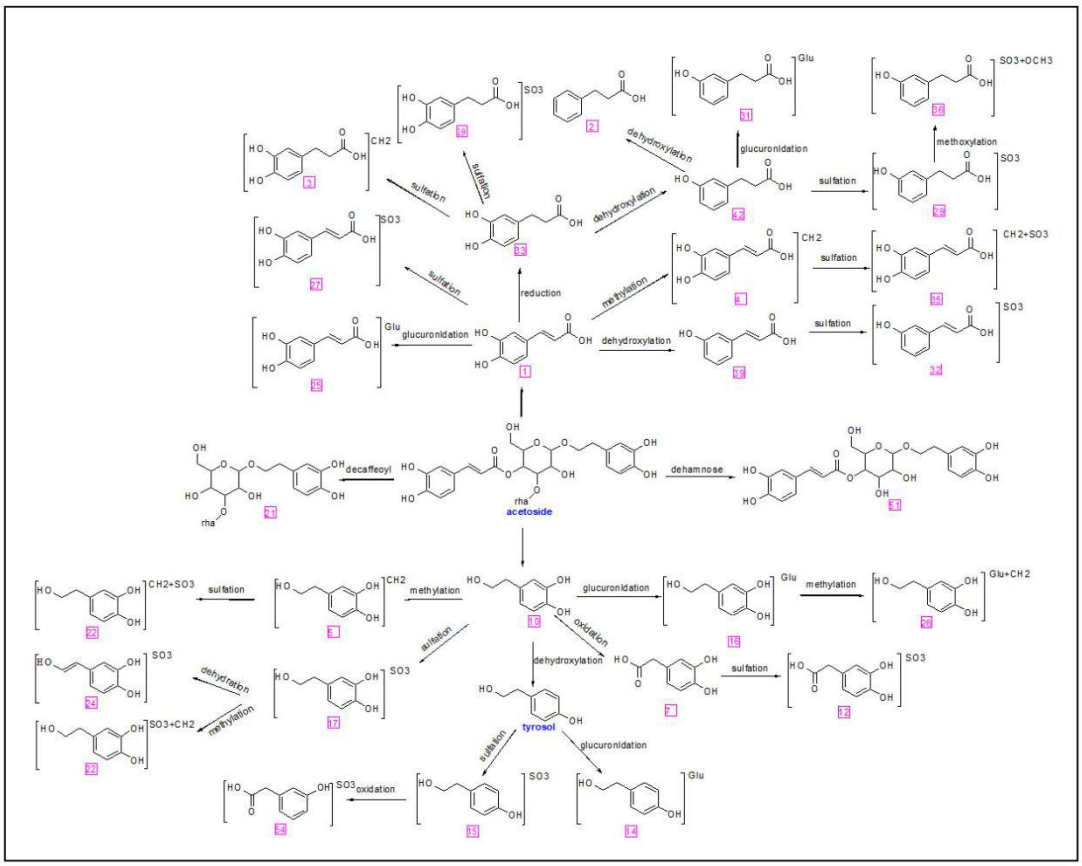

Figure 10 Possible Metabolic pathway of phenylethanoids

Identification of iridoids related metabolites

By analyzing the elemental composition of the metabolites, MS^E fragmentation, and associated literature, a total of 19 iridoid-associated metabolites were tentatively evaluated. Iridoid glycosides are hydrolyzed by glycosidic bonds to form their corresponding aglycones. The *m/z* 185.117 was for M8, 162 Da less than ajugol, was yielded by the loss of glucose residue.

M40 (*m/z*199.0641, Rt 10.91 min) was the deglycosylated product of caalpol. M45 *m/z* 169.0487, Rt 12.15 min) was less than 30 Da that of catalpol deglycosylated metabolite, and was identified as remove a molecule of CH_2O metabolite. M34 (*m/z* 151.0352, Rt 9.08 min), was further loss of H_2O metabolite.

M44 (*m/z* 211.0665, Rt 11.31 min) was a deglycosylated metabolite of geniposide, and M37 (*m/z* 197.0833, Rt 15.03 min) was deglycosylation of 8-epideoxyloganic acid. Metabolic reactions for iridoids could be revealed as phase I metabolism of deglycosylation. Figure 9D.

Comparison of metabolic profiling in plasma, urine, and feces between CD and its processed products

2 prototypes in plasma, 7 in urine, and 3 in feces were compared. There are 7 prototypes absorbed in CD, 7 in CD-NP, and 8 in CD-HP. M21 was only detected in the feces group of CD-NP, and M38 and M51 were detected just in urine groups of CD-HP. Compared with

metabolites, identical metabolites in plasma, urine, and feces were 4, 42, and 21, respectively. There are 34 metabolites absorbed in the CD group, 39 in CD-NP, and 40 in the CD-HP group. M5, M7, M40, and M52 were only detected in CD-NP groups, while M24, M41, and M48 were just detected in CD-HP groups.

In brief, variations were observed in the absorption as well as the metabolism of active compounds in diverse processed products of CD. Furthermore, plasma showed more susceptibility to phase I and then phase II metabolism. Their precursor compounds, such as hydroxytyrosol have anti-tumor, anti-inflammatory, antibacterial, antiviral, and antifungal properties[23]. Caffeic acid possesses anti-inflammatory, anti-cancer, and antiviral activities [24]. It was consistent with the clinical use of CD and its processed products.

Discussion

In TCM clinical practice, the processed products of CD have been widely used relative to raw ones. Up to date, many studies have been carried out for chemical and bio-active evaluation of the raw CD. In the current study, the qualitative analysis of CD, CD-NP and CD-HP was carried out and the obtained results showed variations in the contents of phenylethanoids as well as iridoids during the processing. Under high pressure or steaming (for a long time), glucose-combined phenylethanoids were hydrolyzed, the obtained results showed consistency with the reported studies. *In-vitro* studies revealed variations in chemical composition post-processing, for example, the degradation of few phenylethanoids was carried out, however, elevation was observed in its secondary glycosides or aglycones. While the components showed similarity in CD-NP and CD-HP.

Fragmentation patterns of phenylethanoid glycosides were evaluated by the UPLC-Q-TOF-MS^E technique in negative ion mode. UPLC-Q-TOF-MS^E with UNIFI informatics platform is an analytical method for quick evaluation of chemical ingredients in TCMs sample. In this study, a total of 97 compounds, including phenylethanoid glycosides (PhGs), iridoids, etc. PCA could successfully illustrate the differences for different processing methods samples. CD group was also obviously separated from CD-NP and CD-HP, indicating that these groups could be differentiated. OPLS-DA determined two unique maker ions that could differentiate between CD and processed products. The underlined results indicated that many components were the key characteristic components of each product.

CD is a TCMs and many studies have been reported its key bioactive components, including echinacoside, acteoside, and cistanoside. However, there is a lack of clarity regarding the chemical components absorbed *in vivo* and metabolites post oral administration of CD and its processed products. In the current study, the evaluation of 10 prototype components and 44 metabolites was carried out in urine, plasma, and feces of rats, in which the metabolic processes of phase II were the key cascades and most of the metabolites were sulfate, glucuronide, and methylated conjugates. Phenylethanol glycosides have low oral absorption and utilization. It is difficult to absorb into the

blood, but it can be metabolized by gut flora. Phenylethanol glycosides, the main components in CD, were used as progenitors to play their roles after metabolic activation *in vivo*. Iridoid glycosides, the minor components, are more easily absorbed into the blood after being metabolized into the corresponding aglycone. The metabolism and material basis of CD were preliminarily elucidated. It provides a basis for screening its pharmacodynamic substances and clinical mechanism.

In the current study, most of the metabolites were at lower concentrations or not detected in rat plasma, however, higher concentration was observed in feces or the urine, which indicated that there would be no difficulty in the elimination of underlined metabolites via urine or feces. It indicates that phenylethanolglycosides can degrade rapidly in the gastrointestinal tract after oral administration. Post oral administration of CD and its processed products decoction, phenylethanoids produced into phenylethanolaglycone, like hydroxytyrosine (HT) and caffeic acid (CA) and its derivative 3-hydroxyphenylpropionic acid (3-HPP) through the metabolism of the gastrointestinal tract, these metabolites have the same activity as the prototype. Iridoid glycosides are metabolized as their aglycones. These metabolites may be more easily absorbed into the plasma to have a better medicinal effect. As depicted in Table 3, the same compounds were determined in various groups, while considerable variations were found in the concentrations of the metabolites which might be associated with the unequal efficacy of CD and its processed products.

There were differences of metabolites in urine for CD and its processed products, like methylated HT (M7) and HT oxidation (M5), both were detected only in samples of CD-NP. Decaffeoyl acetoside (M21) and 3,4-dihydroxyphenethyl glycoside (M52) were only detected in feces of CD-NP. Cistanoside F (M49) was detected in feces of CD and CD-NP, whereas cistanoside F reduction (M48) existed in CD-HP. HT sulfate conjugation dehydration product (M24), 6-deoxycatalpol glucuronide conjugation (M41), salidroside (M38) and calceolarisolide A (M51) were only detected in CD-HP.

Generally, the components having high exposure in target organs could be effective. As acteoside and echinacoside are the characteristic compounds in CD, their metabolites may be effective components. A sufficient amount of phenylethanoids and their derivatives have been evaluated and determined *in vitro*, only their degradation products CA and HT derivatives could be evaluated in the bio-samples. The underlined facts reveal that processing can enhance the content of phenylethanoids in CD *in vitro* instead of *in-vivo*. So, it may have preferred to explore a class of compounds relative to a single compound in TCM research.

Conclusion

In the existing study, the detection of 97 compounds was carried out in the extracts of CD and its processed product. Under a high temperature, the degradation of few glycosides was carried out

under an elevated temperature and as a result, some new isomers and complexes were synthesized. In *an in-vivo* study, prototype components (10) and metabolites (44) were determined or tentatively evaluated in rat plasma, feces, and urine. The underlined results revealed that the phase II metabolic processes were the key cascades of each compound and most of the metabolites were associated with echinacoside or acteoside. Numerous metabolites were only determined in rats to post oral administration of CD or CD-NP, and considerable variations were observed in the concentrations of few metabolites. The obtained results showed that the chemical composition of CD was different post-processing and affected the disposition of the compound in *vivo*.

Abbreviations

PhGs: phenylethanoid glycosides; CD: *Cistanche deserticola*; CMM: Chinese Materia Medica; TCM: Traditional Chinese Medicine; CD-NP: *Cistanche deserticola* processed by steaming with rice-wine under normal pressure; CD-HP: *Cistanche deserticola* processed by steaming with rice-wine under high pressure; UPLC-Q-TOF-MS^E: Ultra-high performance liquid chromatography coupled with TOF-MS^E; PCA: principal component analysis; VIP: Variable importance for the projection; CA: Caffeic acid; HA: hydroxytyrosol

Acknowledgements

Not applicable.

Author's contributions

LZ, LBN, SJ participated in drafting, writing the manuscript. RJ, LPP assisted with the animal experiments and drafted and finalized all figures and tables. ZC, HY, JTZ assisted with the design and performance of this study and reviewed the manuscript. All authors approved the final version of the manuscript.

Fundings

This work was supported by the National Natural Science Foundation of China (Grant No: 81874345) and Natural Science foundation of Liaoning Province (Grant No:2020-MS-223).

Availability of data and materials

The datasets used and/or analysed during the current study are available from the corresponding author on reasonale request.

Ethics approval and consent to participate

Ethical approval for using experimental animals for this study had been obtained from the Medical Ethics Committee of Liaoning University of Traditional Chinese Medicine (Approval number:2018YS(DW)-044-01). All experimental procedures in this this study were under ethical standards of the medical Ehtics Committee of Liaoning University of Traditional Chinese Medicine.

Consent for publication

Not applicable.

Competing interests

The Authors declare that they have no conflicts of interest to disclose.

References

[1] Chinese Pharmacopoeia Commission, Pharmacopeia of The People's Republic of China, vol. I, China Medical Science Press, Beijing, 2020, p. 140.

[2] Li Z, Lin H, Gu L, Gao J, Tzeng CM. Herba Cistanche (Rou Cong-Rong): One of the Best Pharmaceutical Gifts of Traditional Chinese Medicine. *Front Pharmacol*, 2016,7:41.

[3] Liu BN, Shi J, Zhang C, Li Z, Hua Y, Liu PP, Jia TZ. Effects of different drying processing methods for Fresh *Cistanche deserticola* on its component contents[J]. *Journal of Chinese Medicinal Materials*, 2020,10:2414-2418.

[4] Liu BN, Shi J, Jia TZ, Lv TT, Li Z. Optimization of high-pressure steaming process for Cistanches Herba[J]. *Chinese Traditional Patent Medicine*,2019,11:2576-2580.

[5] Fan YN, Huang YQ, Jia TZ, Wang J, La Sika, Shi J. Effects of Cistanches herba Before and After Processing on Anti-Aging Function and Immune Function of D-Galactose-Induced Aging Rats[J]. *Chinese Archives of Traditional Chinese Medicine*,2017,11:2882-2885.

[6] Gao YJ, Jiang Y, Dai F, Han ZL, Liu HY, Bao Z, Zhang TM, Tu PF. Study on Laxative Constituents in Cistanche deserticola Y.C.Ma. *Modern Chinese Medicine,* 2015, 17 (4):307-310.

[7] Liu BN, Shi J, Li Z, Zhang C, Liu P, Yao W, Jia T. Study on Neuroendocrine-Immune Function of Cistanche deserticola and Its Rice Wine Steaming Products in Glucocorticoid-Induced Rat Model. *Evid Based Complement Alternat Med.* 2020, 22:5321976.

[8] Guo Y, Wang L, Li Q, Zhao C, He P, Ma X. Enhancement of Kidney Invigorating Function in Mouse Model by Cistanches Herba Dried Rapidly at a Medium High Temperature. *J Med Food.,* 2019, 22(12):1246-1253.

[9] Wang T, Zhang X, Xie W. Cistanche deserticola Y. C. Ma, "Desert ginseng": a review. *Am J Chin Med.* 2012, 40(6):1123-41.

[10] Fu Z, Fan X, Wang X, Gao X. Cistanches Herba: An overview of its chemistry, pharmacology, and pharmacokinetics property. *J Ethnopharmacol*., 2018, 219:233-247.

[11] Lei H, Wang X, Zhang Y, Cheng T, Mi R, Xu X, Zu X, Zhang W. Herba Cistanche (Rou Cong Rong): A Review of Its Phytochemistry and Pharmacology. *Chem Pharm Bull,*2020,68(8):694-712.

[12] Geng X, Tian X, Tu P, Pu X. Neuroprotective effects of echinacoside in the mouse MPTP model of Parkinson's disease. *Eur. J. Pharmacol.,* 2007,564 :66-74.

[13] Deng M, Zhao JY, Ju XD, Tu PF, Jiang Y, Li ZB. Protective effect of tubuloside B on TNF alpha-induced apoptosis in neuronal cells. *Acta Pharmacol Sin.*,2004,25(10):1276-84.

[14] Nan ZD, Zhao MB, Zeng KW, Tian SH, Wang WN, Jiang Y, Tu PF. Anti-inflammatory iridoids from the stems of *Cistanche deserticola* cultured in Tarim Desert. *Chin J Nat Med.* 2016, 14(1):61-5.

[15] Nan ZD, Zeng KW, Shi SP, Zhao MB, Jiang Y, Tu PF. Phenylethanoid glycosides with anti-inflammatory activities from the stems of Cistanche deserticola cultured in Tarim desert. *Fitoterapia*. 2013,89:167-74.

[16] Morikawa T, Pan Y, Ninomiya K, Imura K, Yuan D, Yoshikawa M, Hayakawa T, Muraoka O. Iridoid and acyclic monoterpene glycosides, kankanosides L, M, N, O, and P from *Cistanche tubulosa*. *Chem Pharm Bull* , 2010, 58(10):1403-7.

[17] Li SL, Song JZ, Qiao CF. *et al*. A novel strategy to rapidly explore potential chemical markers for the discrimination between raw and processed Radix Rehmanniae by UHPLC-TOF-MS with multivariate statistical analysis [J]. *J Pharm Biomed Anal*, 2010, 51(4): 812-823.

[18] Peng F, Chen J, Wang X, Xu CQ, Liu TN, Xu R. Changes in levels of phenylethanoid glycosides, antioxidant activity, and other quality traits in *Cistanche deserticola* slices by steam processing. *Chem. Pharm. Bull.*, 2016, 64, 1024–1030.

[19] Ma ZG, Tan YX. Contents changes of six phenylethanoid glycosides under steaming time spans with wine in

Desertliving Cistanche.*Chinese Traditional Patent Medicine.*2011,33(11):1951-1954.

[20] Peng F, Xu R, Wang X, Xu C, Liu T, Chen J. Effect of the Steaming Process on Quality of Postharvest Cistanche deserticola for Medicinal Use during Sun Drying. *Biol Pharm Bull.* 2016;39(12):2066-2070.

[21] Cui Q, Pan Y, Zhang W, Zhang Y, Ren S, Wang D, Wang Z, Liu X, Xiao W. Metabolites of Dietary Acteoside: Profiles, Isolation, Identification, and Hepatoprotective Capacities. *J Agric Food Chem.* 2018, 66(11):2660-2668.

[22] Cui Q, Pan Y, Bai X, Zhang W, Chen L, Liu X. Systematic characterization of the metabolites of echinacoside and acteoside from Cistanche tubulosa in rat plasma, bile, urine and feces based on UPLC-ESI-Q-TOF-MS. *Biomed Chromatogr,* 2016,30(9):1406-15.

[23] Bertelli M, Kiani AK, Paolacci S, Manara E, Kurti D, Dhuli K, Bushati V, Miertus J, Pangallo D, Baglivo M, Beccari T, Michelini S. Hydroxytyrosol: A natural compound with promising pharmacological activities. *J Biotechnol.* 2020, 309:29-33.

[24] Touaibia M, Jean-François J, Doiron J. Caffeic Acid, a versatile pharmacophore: an overview. *Mini Rev Med Chem.* 2011,11(8):695-713.

Figures

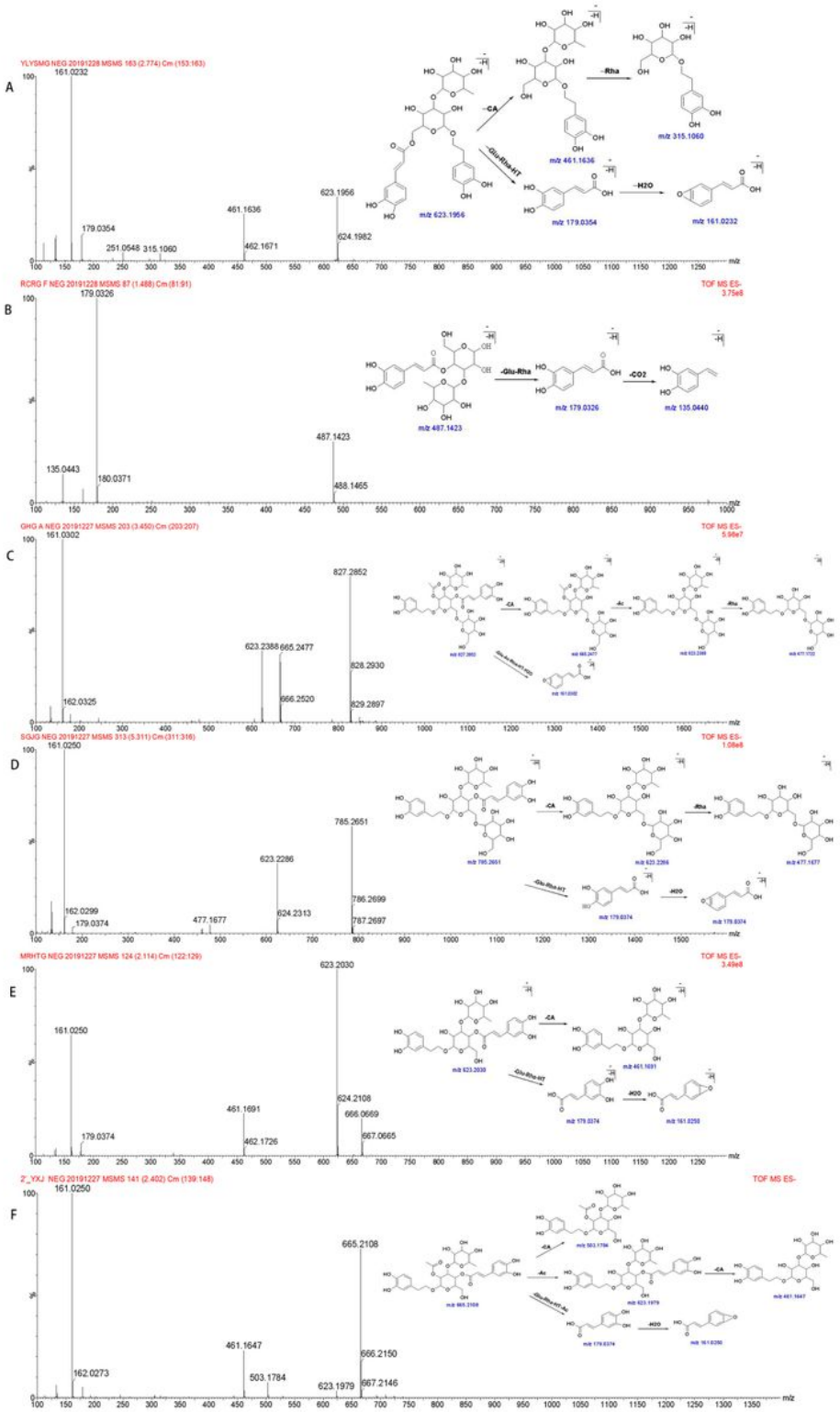

Figure 1

A.isoacteoside; B.cistanosideF; C.tubulosideA; D.echinacteoside; E. acteoside; F.2'-actylacteoside Mass Spectrogram and cleavage pathway of phenylethanoid glycosides

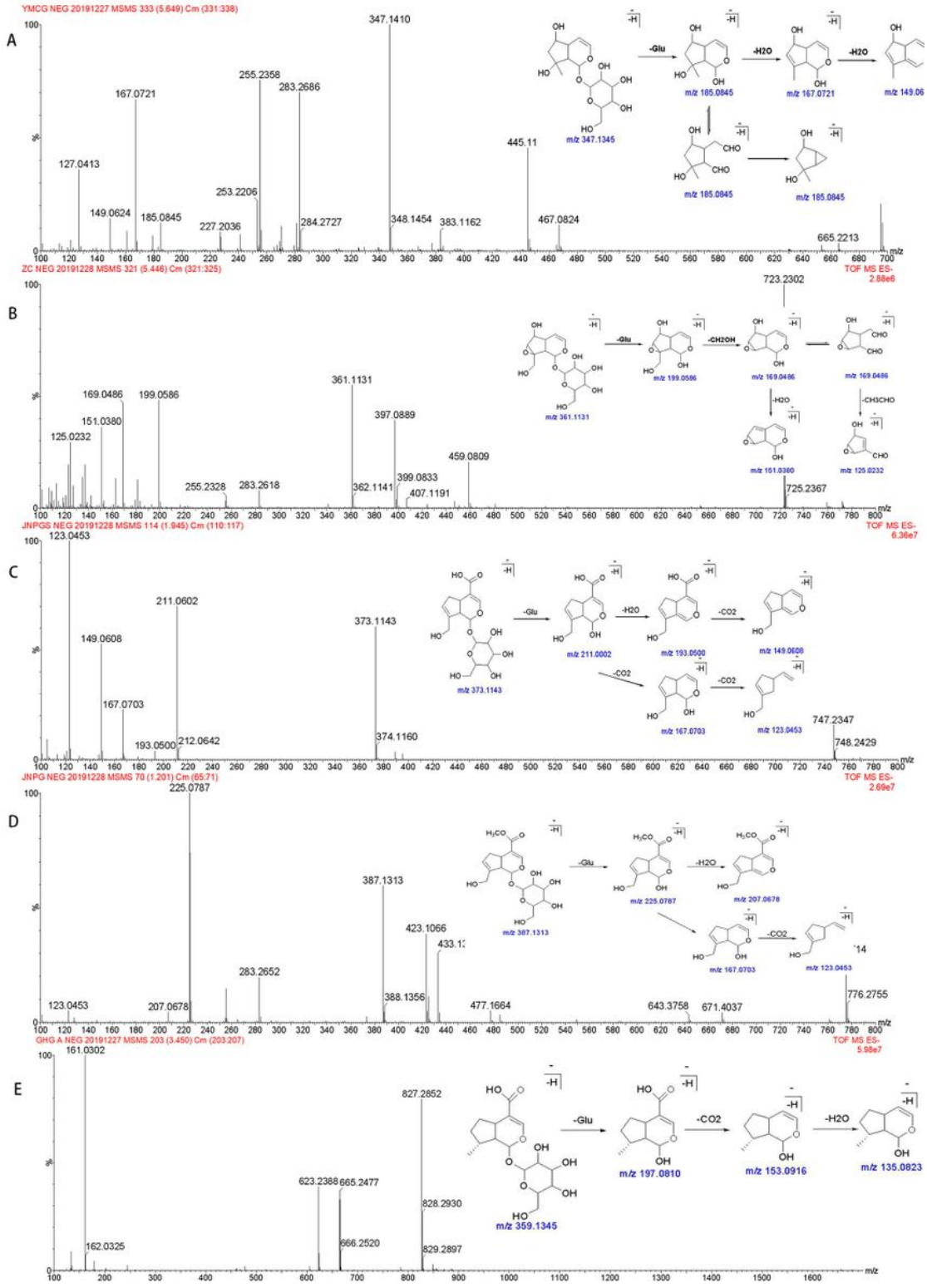

Figure 2

A.ajugol B.catalpol C.geniposidic acid D. geniposide E.8-epideoxyloganic acid Mass Spectrogram and cleavage pathway of iridoid

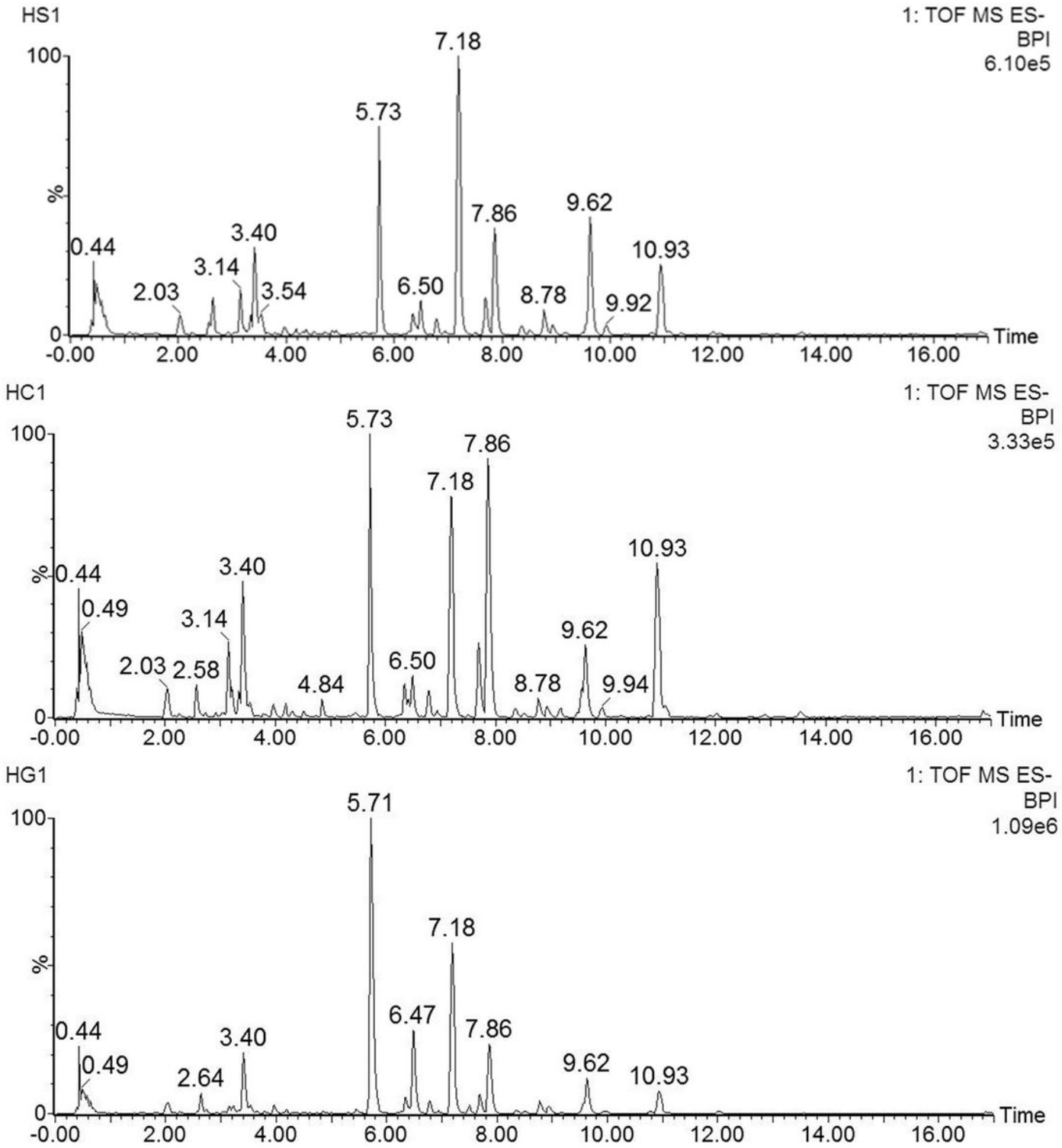

Figure 3

1.CD, 2. CD-NP, 3. CD-HP The base peak intensity (BPI) of the samples

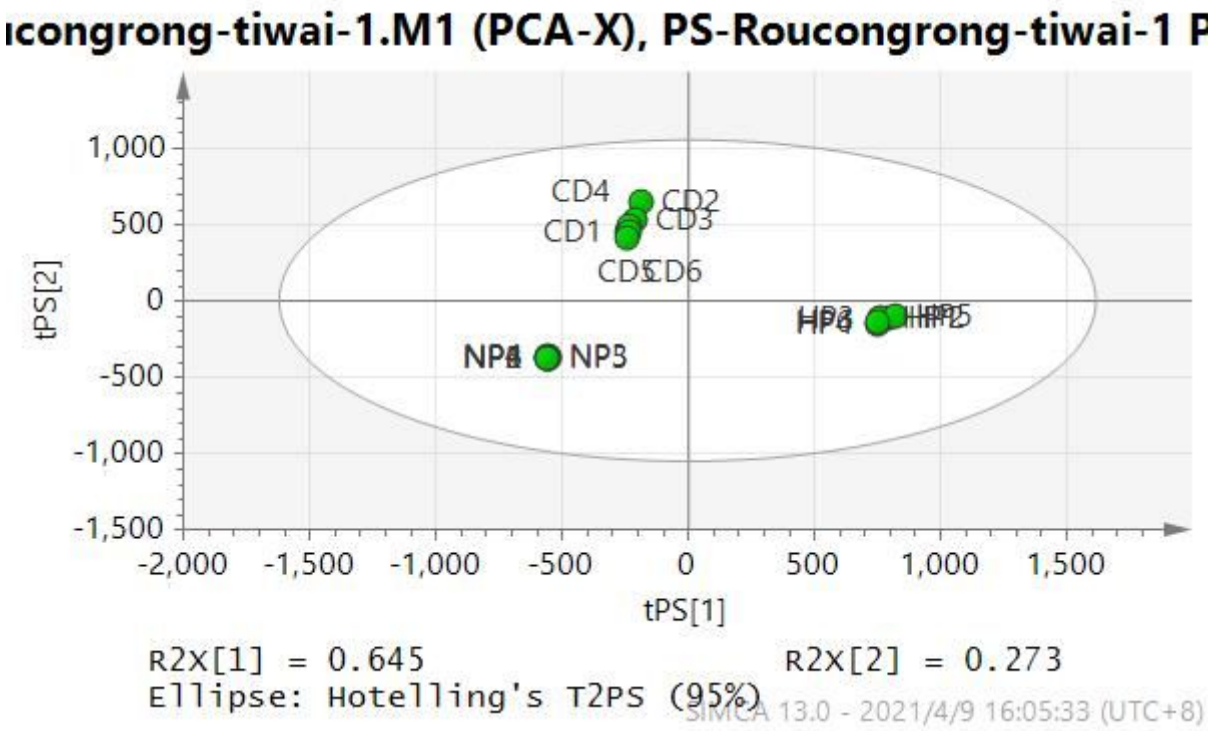

Figure 4

The PCA of CD and its different processed pro

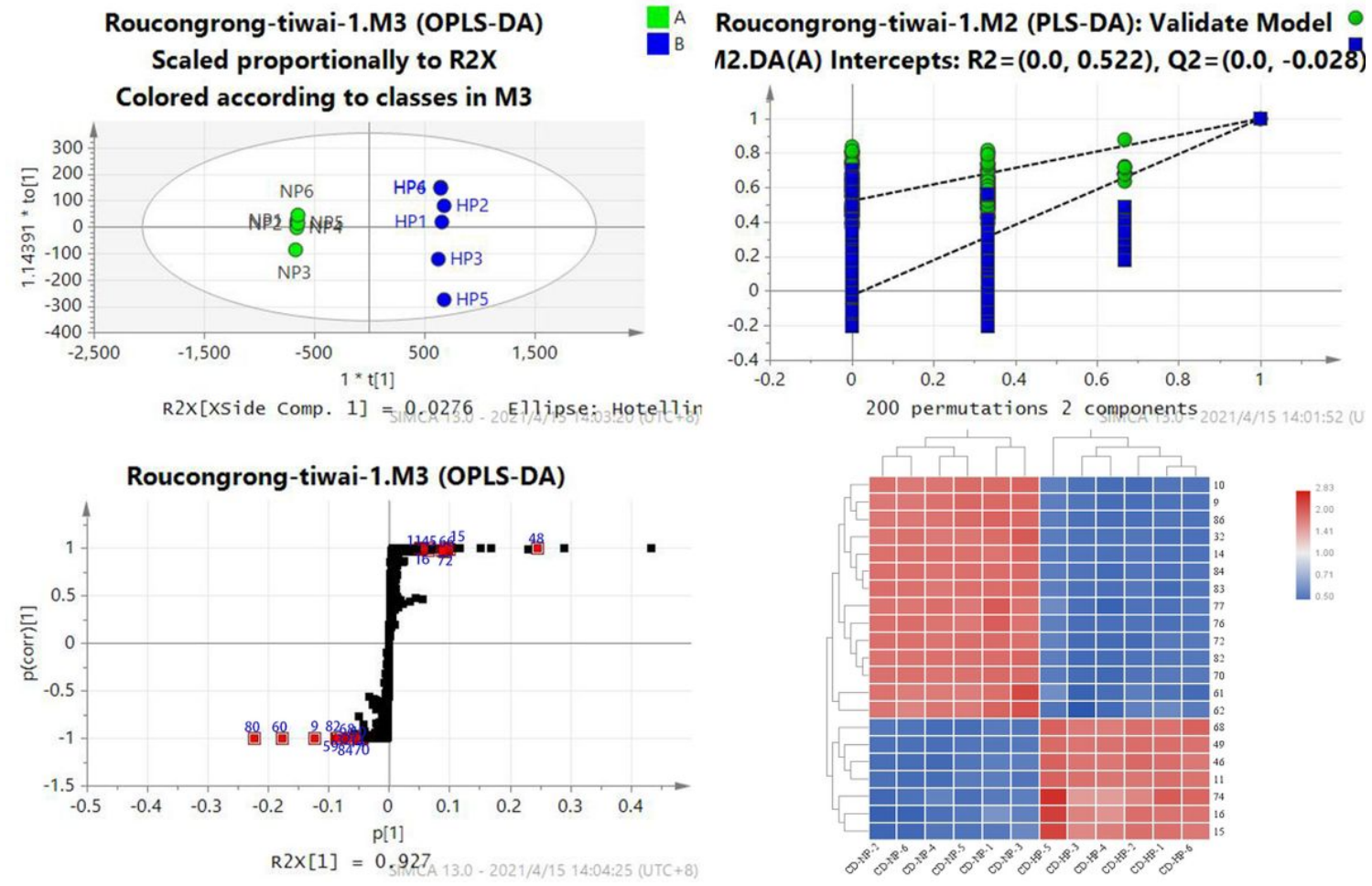

Figure 5

The OPLS-DA/permutation test/S-plot /heat map indicating the intensities of potential biomarkers between CD-NP and CD-HP

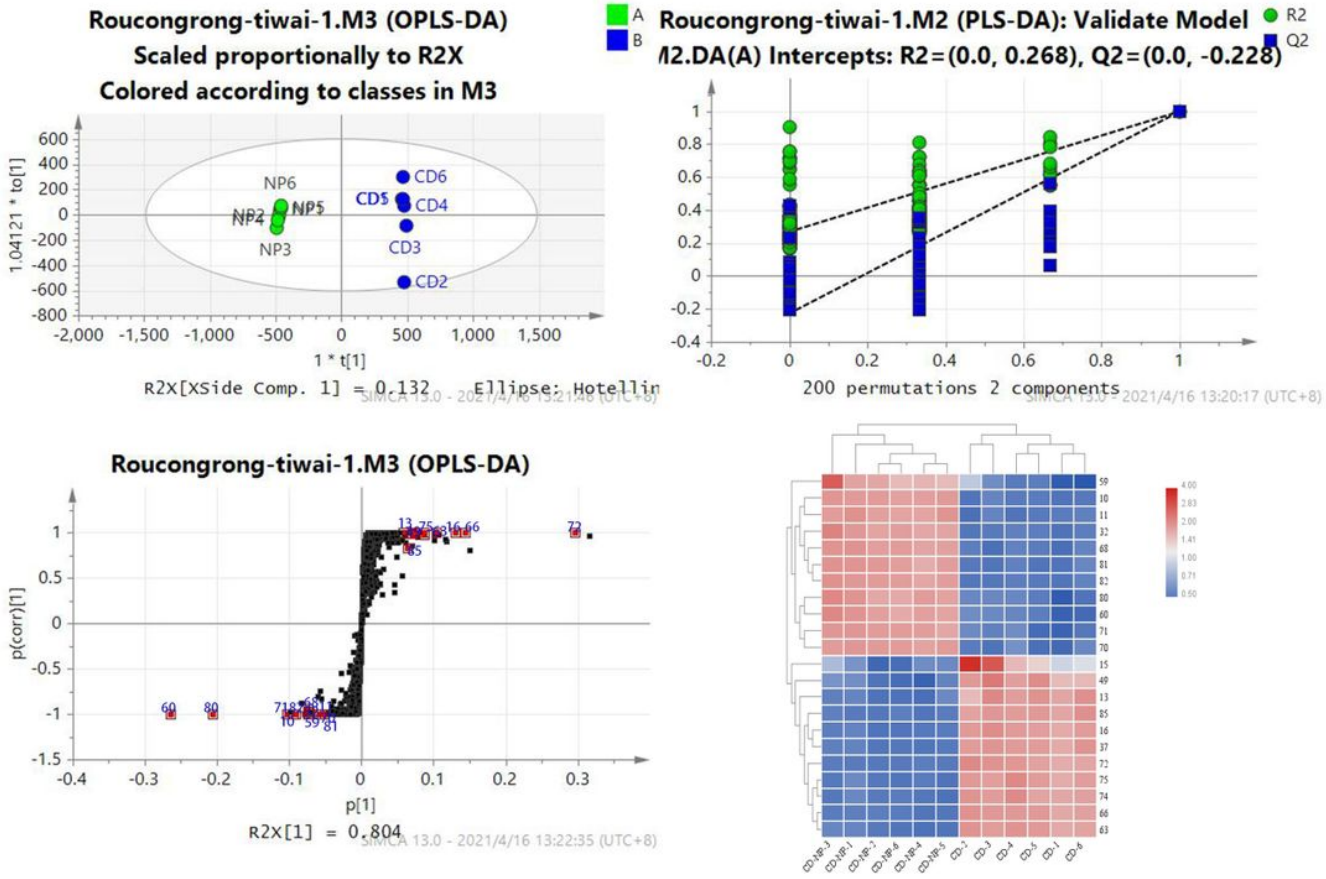

Figure 6

The OPLS-DA /permutation test/ S-plot/ heatmaps indicating the intensities of effective biomarkers between CD and CD-N

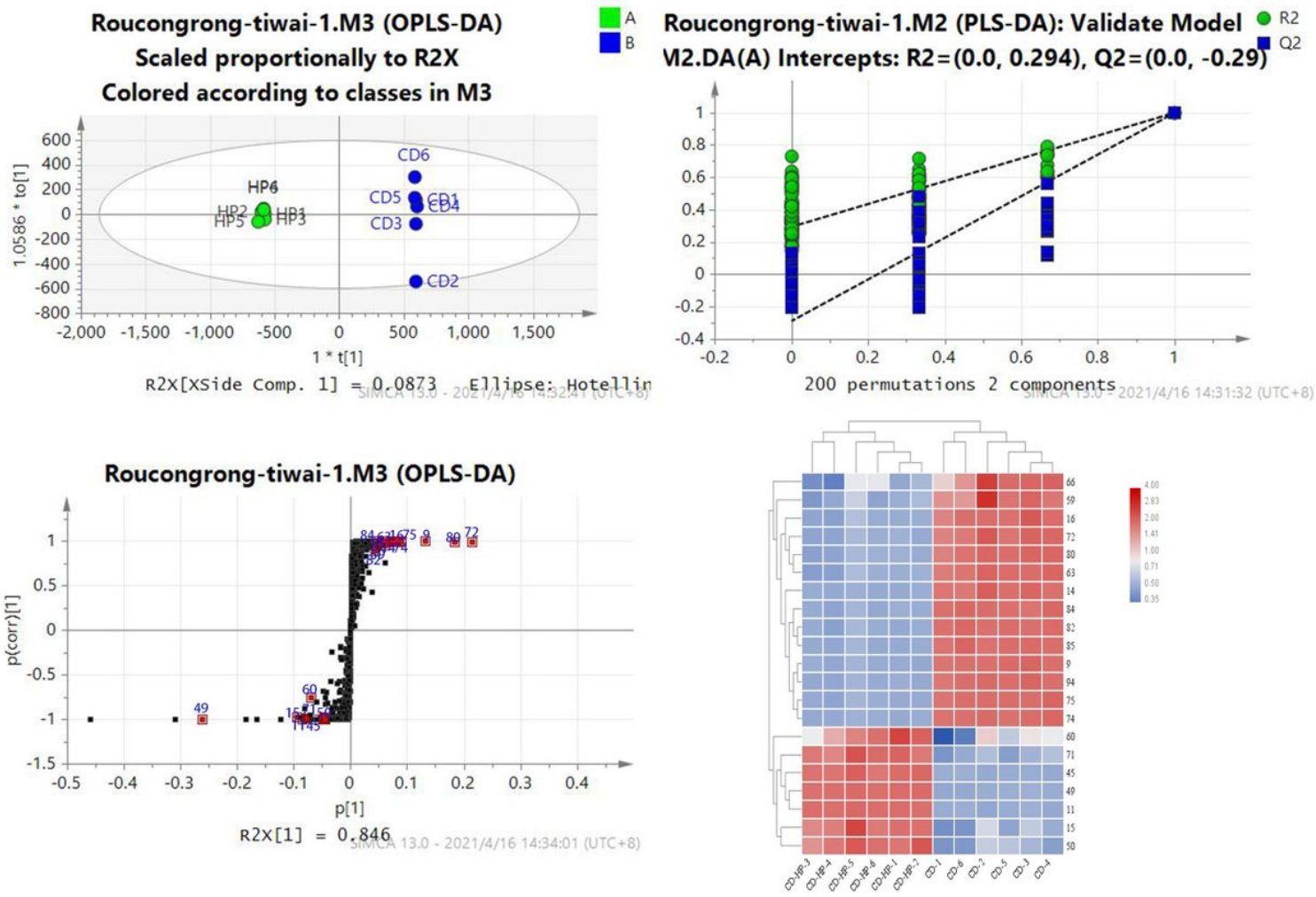

Figure 7

The OPLS-DA/permutation test/S-plot/ heatmaps revealing the intensities of effective biomarkers between CD and CD-HP

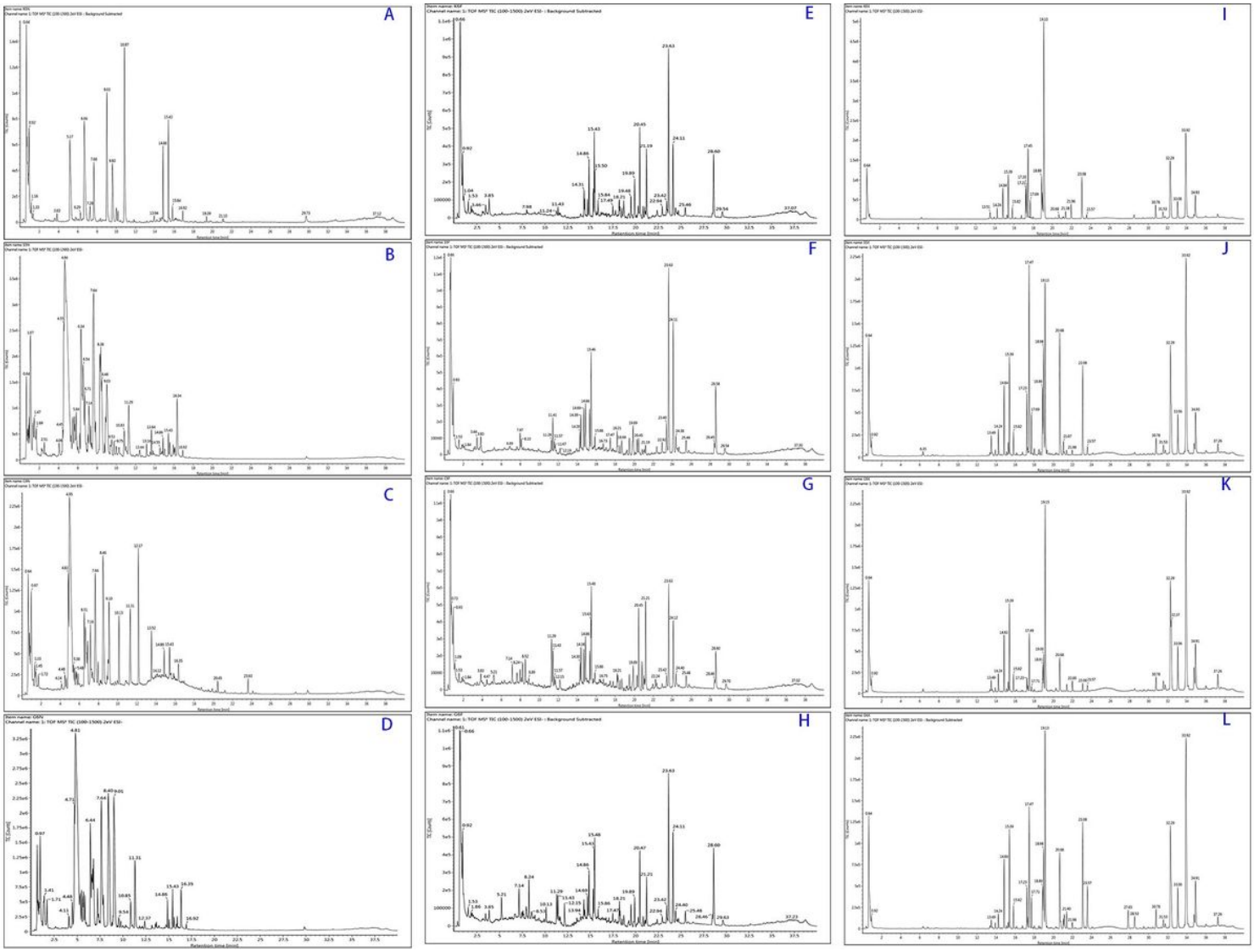

Figure 8

A. Urine sample in BC group; B. Urine sample in CD group; C. Urine sample in CD-NP group; D. Urine sample in CD-HP group; E. Feces sample in BC group; F. Feces sample in CD group; G. Feces sample in CD-NP group; H. Feces sample in CD-HP group; I. Plasma sample in BC group; J. Plasma sample in CD group; K. Plasma sample in CD-NP group; M. Plasma sample in CD-HP group chromatograph of TIC

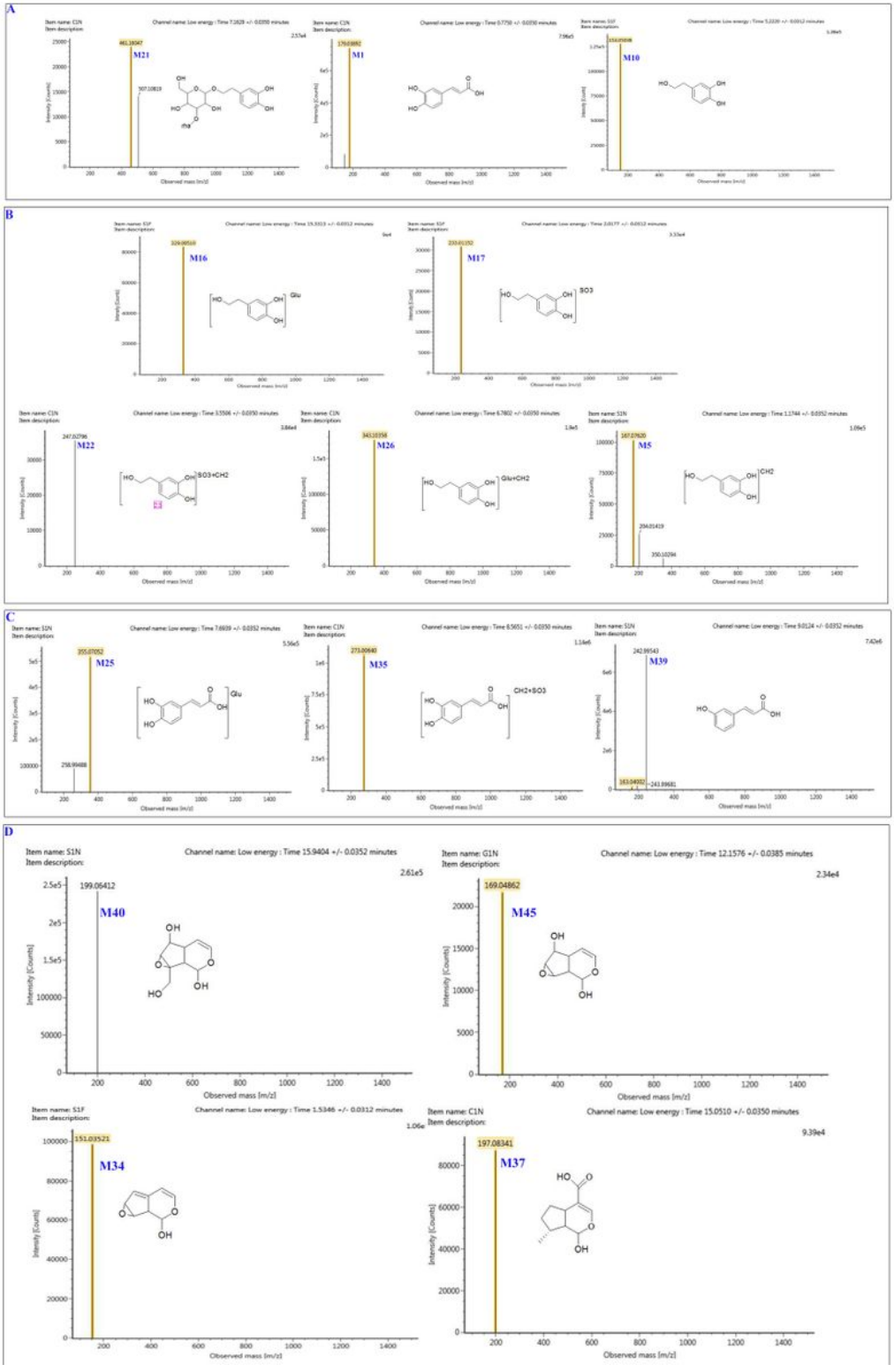

Figure 9

Mass Spectrum of some Metabolites in CDs

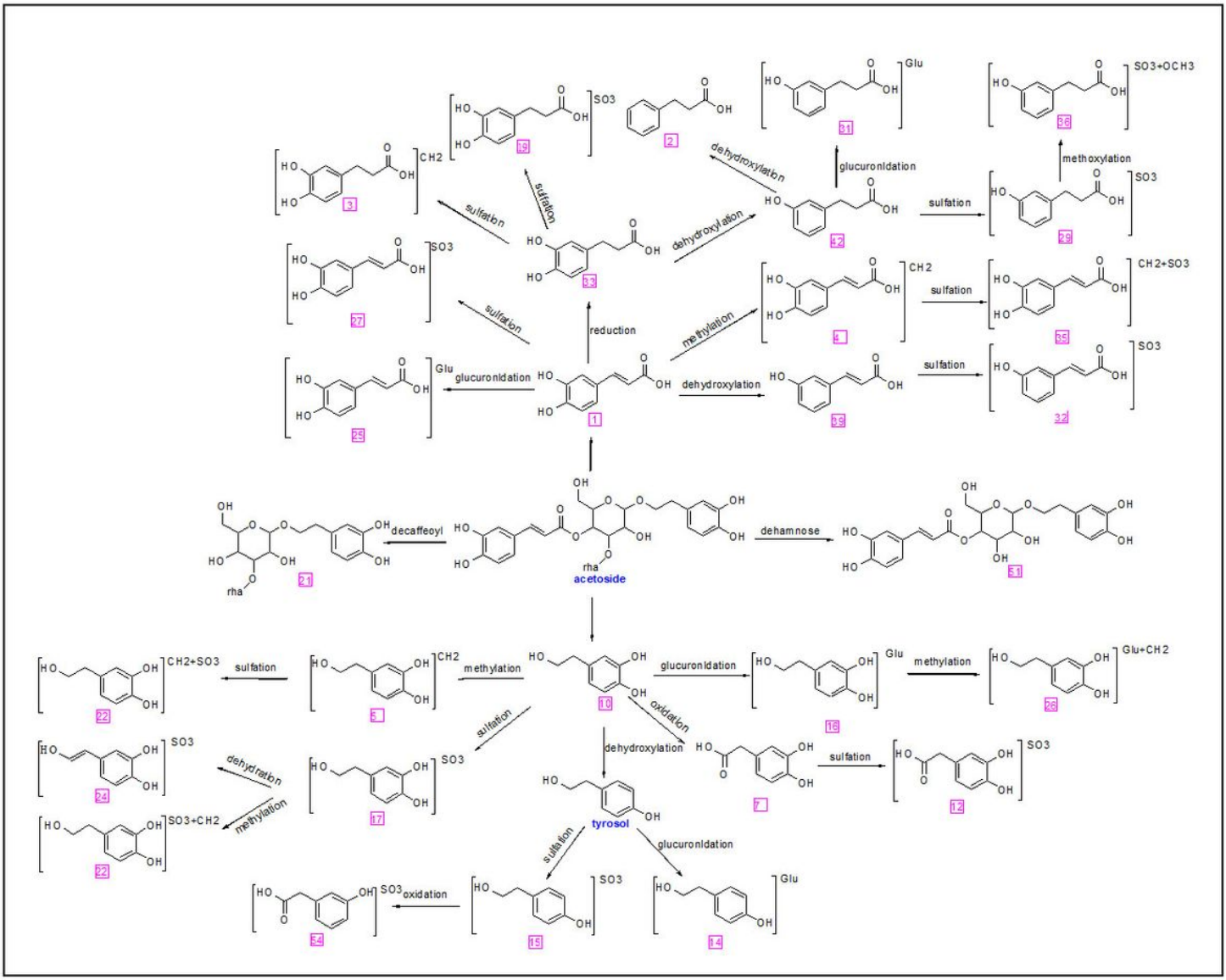

Figure 10

Possible Metabolic pathway of phenylethanoids